

Low-Melting, Low-Viscous, Hydrophobic Ionic Liquids: 1-Alkyl(Alkyl Ether)-3-methylimidazolium Perfluoroalkyltrifluoroborate

Zhi-Bin Zhou, Hajime Matsumoto,* and Kuniaki Tatsumi^[a]

Abstract: A series of twenty two hydrophobic ionic liquids, 1-alkyl(alkyl ether)-3-methylimidazolium ($[C_m\text{mim}]^+$ or $[C_mO_n\text{mim}]^+$; where C_m is 1-alkyl, $C_m = nC_mH_{2m+1}$, $m = 1-4$ and 6; C_mO_n is 1-alkyl ether, $C_2O_1 = \text{CH}_3\text{OCH}_2$, $C_3O_1 = \text{CH}_3\text{OCH}_2\text{CH}_2$, and $C_5O_2 = \text{CH}_3(\text{OCH}_2\text{CH}_2)_2$) perfluoroalkyltrifluoroborate ($[\text{R}_F\text{BF}_3]^-$, $\text{R}_F = \text{CF}_3$, C_2F_5 , $n\text{C}_3\text{F}_7$, $n\text{C}_4\text{F}_9$), have been prepared and characterized. Some of the important

physicochemical properties of these salts including melting point, glass transition, viscosity, density, ionic conductivity, thermal and electrochemical stability, have been determined and were compared with those of the reported

Keywords: electrolytes • ionic liquids • perfluoroalkyltrifluoroborate • phase transitions • viscosity

$[\text{BF}_4]^-$ -based ones. The influence of the structure variation in the imidazolium cation and the perfluoroalkyltrifluoroborate ($[\text{R}_F\text{BF}_3]^-$) anion on the above physicochemical properties was discussed. The key features of these new salts are their low melting points (-42 to 35°C) or extremely low glass transition (between -87 and -117°C) without melting, and considerably low viscosities ($26-77$ cP at 25°C).

Introduction

Room temperature ionic liquids are salts composed entirely of large organic cations, in particular 1,3-dialkylimidazolium cations, and a wide variety of anions, and usually having a melting point at or below room temperature (25°C). In recent years, ionic liquids (ILs) have attracted an increasing interest for application as new media in organic reactions,^[1] biocatalytic transformations,^[2] and separation technologies,^[3] and as potential electrolytes in various electrochemical devices and electroplating,^[4] and so on, which have been intensively reviewed. The obvious advantages of ILs over conventional organic solvents and electrolytes are their nonflammability, nonvolatility, high thermal stability and a wide stable liquid range (usually over 200°C).^[1-5] The most attractive features of ILs is that their physical and chemical properties, such as melting point, density, viscosity, hydrophobicity and coordinating ability, can be finely tuned by alteration of the cation or anion to specific applications; hence ILs have been referred to as “designer solvents” or “tailored solvents”.^[1c,d]

In spite of all the aforementioned advantages, ILs still have many barriers to overcome before they can be widely

used in industry to replace the conventional organic solvents or electrolytes. One of the severe barriers associated with the application of ILs is the inherently high viscosity of ILs, usually being two or three orders of magnitude greater than those of water and conventional organic solvents (e.g. 1 cP for water and 0.59 cP toluene at 20°C).^[1c,d,4b] The high viscosity not only negatively affects power requirements and handling (dissolution, decantation, filtration, etc.) but also leads to the reduction of the reaction rate.^[6] So far, a large number of new ionic liquids have been reported,^[4c] however, most of them are high-viscous and/or high-melting while the low-viscous ones are rather rare. Among the ILs reported, the most fluid ILs (<45 cP at 25°C) have been usually obtained by combining 1-ethyl-3-methylimidazolium ($[C_2\text{mim}]^+$) cation with some specific anions, such as fluorohydrogenate ($[\text{F}(\text{HF})_{2,3}]^-$, 4.8 cP),^[7] chloroaluminates (18 cP for $[\text{AlCl}_4]^-$ and 14 cP for $[\text{Al}_2\text{Cl}_7]^-$),^[8] dicyanamide ($[\text{N}(\text{CN})_2]^-$, 17–21 cP),^[9,10] tricyanomethanide ($[\text{C}(\text{CN})_3]^-$, 18 cP at 22°C),^[10,11] 2,2,2-trifluoro-*N*-(trifluoromethylsulfonyl)acetamide ($[(\text{CF}_3\text{SO}_2)(\text{CF}_3\text{CO})\text{N}]^-$, 25 cP),^[12] bis(trifluoromethylsulfonyl)imide ($[(\text{CF}_3\text{SO}_2)_2\text{N}]^-$, 28 cP),^[13,14] tetrafluoroborate ($[\text{BF}_4]^-$, 37–43 cP),^[13,15] and so on. However, most of these low-viscous ILs are still of limited application because of the less suitability of the anion counterparts: $[\text{AlCl}_4]^-$ and $[\text{Al}_2\text{Cl}_7]^-$ are well-known for their moisture sensitivity and high reactivity, $[\text{F}(\text{HF})_{2,3}]^-$ are reactive and less thermally stable (ca. 80°C),^[8b,16] $[\text{N}(\text{CN})_2]^-$ and $[\text{C}(\text{CN})_3]^-$ exhibit somewhat coordinating ability that might inactivate the catalysts in organic reactions,^[9a] and $[(\text{CF}_3\text{SO}_2)(\text{CF}_3\text{CO})\text{N}]^-$ and $[(\text{CF}_3\text{SO}_2)_2\text{N}]^-$ for ILs may be

[a] Dr. Z.-B. Zhou, Dr. H. Matsumoto, Dr. K. Tatsumi
Research Institute for Ubiquitous Energy Devices
National Institute of Advanced Industrial Science
and Technology (AIST)
1-8-31 Midorigaoka, Ikeda, Osaka 563-8577 (Japan)
Fax: (+81) 72-727-9622
E-mail: h-matsumoto@aist.go.jp

too expensive. Thus, the easily available but relatively high-viscous $[\text{BF}_4]^-$ -based ILs still remain in an unchallenged position in the field of ILs because of their good chemical, electrochemical, and thermal stabilities, and the well-established preparation processes.^[13, 15, 17–20] However, the low-viscous $[\text{C}_2\text{mim}][\text{BF}_4]$ is usually contaminated by halide impurities arising from the preparation process (i.e., metathesis reaction between $[\text{C}_2\text{mim}]\text{X}$ ($\text{X} = \text{Cl}^-, \text{Br}^-$) and silver or ammonium salts of the $[\text{BF}_4]^-$),^[15, 17, 21] which are very difficult to be removed by conventional purification process and have severely deleterious effects if used as a solvent in catalytic and biocatalytic reactions.^[21, 22] Consequently, a remarkably high-viscous salt, 1-butyl-3-methylimidazolium tetrafluoroborate ($[\text{C}_4\text{mim}][\text{BF}_4]$, about 180 cP at 25 °C^[15c]), is most commonly preferred to the $[\text{C}_2\text{mim}][\text{BF}_4]$ in recent studies,^[1d] because the former is more hydrophobic than the latter, and this allowing to remove water-soluble impurities such as halide ions from the former by washing with water.^[17, 18] With the rapidly expanding applications of ILs in various fields, there obviously exists a significant need for the preparation of new hydrophobic, low-melting, and low-viscous ionic liquids.

Recently a new class of weakly coordinating fluoroanions, namely perfluoroalkyltrifluoroborates ($[\text{R}_\text{F}\text{BF}_3]^-$), have been successfully synthesized via various convenient methods,^[23–27] whose chemistry and application in high-energy devices, such as Li-ion batteries and electrochemical double-layer capacitors, are currently of great interest because of their good chemical and electrochemical stability.^[27, 28] More recently, several ILs based on the $[\text{R}_\text{F}\text{BF}_3]^-$ have also been reported in two limited studies.^[29] As part of our interest to find new ILs, we herein systematically report the synthesis and characterization of a series of twenty two low-melting, low-viscous, and hydrophobic ILs based on the 1-alkyl(alkyl ether)-3-methylimidazolium ($[\text{C}_m\text{mim}]^+$ or $[\text{C}_m\text{O}_n\text{mim}]^+$; wherein C_m is 1-alkyl, $\text{C}_m = n\text{C}_m\text{H}_{2m+1}$, $m = 1–4$ and 6; C_mO_n is 1-alkyl ether, $\text{C}_2\text{O}_1 = \text{CH}_3\text{OCH}_2$, $\text{C}_3\text{O}_1 = \text{CH}_3\text{OCH}_2\text{CH}_2$, and $\text{C}_5\text{O}_2 = \text{CH}_3(\text{OCH}_2\text{CH}_2)_2$) and perfluoroalkyltrifluoroborate ($[\text{R}_\text{F}\text{BF}_3]^-$, $\text{R}_\text{F} = \text{CF}_3$, C_2F_5 , $n\text{C}_3\text{F}_7$, $n\text{C}_4\text{F}_9$), as well as their electrochemical properties including ionic conductivity and electrochemical stability.

Results and Discussion

The structures and abbreviations of the cation and anion employed in the present study are displayed in Table 1, and the ILs based on these cations and anions are shown in Table 2 (entries 1–22). All the $[\text{R}_\text{F}\text{BF}_3]^-$ -based salts in Table 2 were prepared by metathesis reactions of the corresponding imidazolium halide with a little excess of $\text{K}[\text{R}_\text{F}\text{BF}_3]$ (1.05 equiv) in water at room temperature, followed by simply washing with water to remove water-soluble impurities, because they are immiscible with water to some extent. All the salts prepared were characterized by ^1H , ^{19}F , and ^{11}B NMR, FAB-MS, and elemental analysis. The characterization data are in agreement well with the expected structures and compositions. The final yields of these salts were over a range from moderate to high (60–95 %).

Generally, increasing the length of the 1-alkyl (C_m) chain in the cation or perfluoroalkyl (R_F) chain in the $[\text{R}_\text{F}\text{BF}_3]^-$ resulted in an increase in yield; however, replacing the 1-alkyl (C_m) group with the hydrophilic alkyl ether (C_mO_n) group decreased the yields (60–68 %).

It has been identified that the chemical and physical properties of ILs can be drastically altered by the presence of small amounts of impurities, notably residual halide and water, arising from the preparation process.^[20, 21] Therefore, the contents of water and halide ions in the resulting salts were determined. The water content in the $[\text{R}_\text{F}\text{BF}_3]^-$ -based salts was revealed to be less than 50 ppm after vacuum drying at 70 °C for 24 h because of their hydrophobicity, whereas the hydrophilic $[\text{C}_2\text{mim}][\text{BF}_4]$ still contained about 200 ppm of water after drying under the same conditions. The amount of residual halide and potassium ions in the $[\text{R}_\text{F}\text{BF}_3]^-$ -based salts, determined by fluorescence X-ray spectrometry, was less than 50 ppm. More importantly, in all the $[\text{R}_\text{F}\text{BF}_3]^-$ -based salts, F^- (HF) content determined by ion chromatography was lower than 5 ppm; this indicates that the $[\text{R}_\text{F}\text{BF}_3]^-$ is stable toward hydrolysis during the preparation process probably owing to their hydrophobicity. On the other hand, a high content of about 240 ppm F^- (HF) in the hydrophilic $[\text{C}_2\text{mim}][\text{BF}_4]$ was detected, strongly indicating that a trace amount of $[\text{BF}_4]^-$ hydrolyzed during the preparation process, and the $[\text{BF}_4]^-$ is therefore less stable against hydrolysis than the $[\text{R}_\text{F}\text{BF}_3]^-$. Moreover, the rapid hydrolysis of the $[\text{BF}_4]^-$ was also observed for the $[\text{C}_4\text{mim}][\text{BF}_4]$ when this salt was dissolved in the mixture solvents of water/methanol.^[21d] All these observations suggest that the hydrophilic $[\text{BF}_4]^-$ -based ILs, such as $[\text{C}_2\text{mim}][\text{BF}_4]$, are evidently not inert in the presence of water, although they are widely described as moisture stable ILs in a number of literatures.

The physicochemical properties of these prepared salts were characterized by differential scanning calorimetry (DSC), thermal gravimetric analysis (TGA), density (d), dynamic viscosity (η), ionic conductivity (κ). The characterization data are summarized in Table 2. The data for three of these salts, $[\text{C}_2\text{mim}][\text{R}_\text{F}\text{BF}_3]$ ($\text{R}_\text{F} = \text{C}_2\text{F}_5$, $n\text{C}_3\text{F}_7$, $n\text{C}_4\text{F}_9$), agree well with a recent report,^[29a] where they were prepared by a halide-free route with high purity. These results further suggest that the purities of the salts prepared in the present study are of high grade, and the characterization data are not in error. For comparison, four of the reported $[\text{BF}_4]^-$ -based salts,^[15, 17, 18, 20] $[\text{C}_m\text{mim}][\text{BF}_4]$ ($m = 2, 3, 4, 6$), are also included in Table 2.

Phase transition: The solid–liquid phase transitions of these new salts were investigated using differential scanning calorimetry (DSC) from -150°C to the melting point. One of the significant features for these new salts is that many of them exhibit glass-forming characteristics. In addition, four of these salts showed a solid–solid transition (see Table 2, $T_{\text{s-s}}$ for entries 17, 18, 20, and 22) before melting. The respective melting entropies for these four salts were 33.1, 34.9, 30.2, and 72.2 $\text{JK}^{-1}\text{mol}^{-1}$. These results suggest that the first three salts (entries 17, 18, and 20) may show some extents of ionic plastic behavior because their melting entropies

Table 1. Structure of ionic liquids 1-alkyl(alkyl ether)-3-methylimidazolium perfluoroalkyltrifluoroborate ($[C_m\text{mim}][R_f\text{BF}_3]$ and $[C_m\text{O}_n\text{mim}][R_f\text{BF}_3]$).

Cation	R	Anion
$[C_1\text{mim}]^+$	CH ₃	$[\text{CF}_3\text{BF}_3]^-$
$[C_2\text{mim}]^+$	C ₂ H ₅	$[\text{C}_2\text{F}_5\text{BF}_3]^-$
$[C_3\text{mim}]^+$	<i>n</i> C ₃ H ₇	$[n\text{C}_3\text{F}_7\text{BF}_3]^-$
$[C_4\text{mim}]^+$	<i>n</i> C ₄ H ₉	$[n\text{C}_4\text{F}_9\text{BF}_3]^-$
$[C_6\text{mim}]^+$	<i>n</i> C ₆ H ₁₃	
$[C_2\text{Omim}]^+$	CH ₃ OCH ₂	
$[C_3\text{Omim}]^+$	CH ₃ O(CH ₂) ₂	
$[C_5\text{O}_2\text{mim}]^+$	CH ₃ O(CH ₂) ₂ O(CH ₂) ₂	

pies were $<40 \text{ J K}^{-1} \text{ mol}^{-1}$, which are very close to the melting entropy of the ionic plastic crystal based on the large flexible anion $[(\text{CF}_3\text{SO}_2)_2\text{N}]^-$ ($\Delta S = 40 \text{ J K}^{-1} \text{ mol}^{-1}$).^[4b,31] Figure 1 shows the DSC traces of four representatives (Table 2, entries **1**, **2**, **5**, and **18**) as examples, where a range of phase transitions for all the salts in the present study are included.

For the imidazolium-based salts, the influence of structure variation in the cation and anion on the melting point has been widely investigated previously.^[14,17,20,32] Qualitatively, low symmetry, weak ion interactions (such as suppressing hydrogen-bonding) and effective charge distribution over the cation and/or anion tends to reduce the crystal lattice

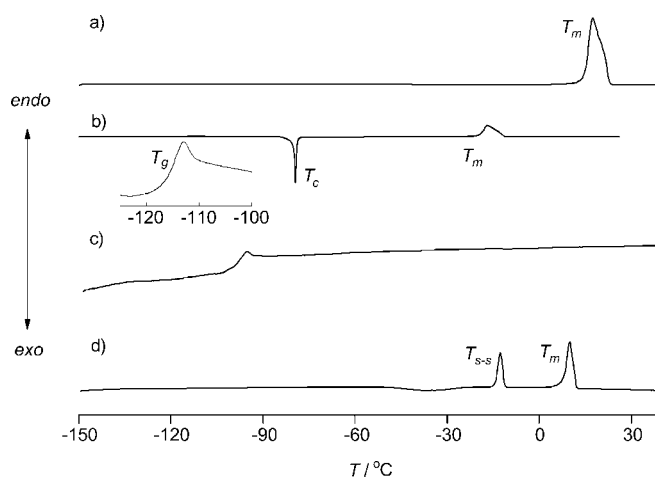


Figure 1. DSC traces (heating) for a) $[C_1\text{mim}][\text{CF}_3\text{BF}_3]$, b) $[C_2\text{mim}][\text{CF}_3\text{BF}_3]$, c) $[C_6\text{mim}][\text{CF}_3\text{BF}_3]$, and d) $[C_2\text{mim}][n\text{C}_3\text{F}_7\text{BF}_3]$; inset is an enlarged trace for b) $[C_2\text{mim}][\text{CF}_3\text{BF}_3]$ in the low temperature range around T_g .

energy of the salts, thus resulting in low-melting salts. However, the exact reason many imidazolium salts are low-melting is still not well understood, but it is believed to be a combination of the competing influences of ion-ion and van der Waals interactions and the disruption of Coulombic packing.^[14,17,20,32,33]

Figure 2 shows the observed melting points (T_m) of these new salts including those of the salts with $[\text{BF}_4]^-$ for compar-

Table 2. Physicochemical properties of the salts prepared (water content in all the salts <50 ppm, with the exception of ca. 200 ppm water in the $[C_2\text{mim}][\text{BF}_4]$).

Entry	Salts	T_g [°C] ^[a]	T_c [°C] ^[b]	T_{s-s} [°C] ^[c]	T_m [°C] ^[d]	T_d [°C] ^[e]	d [g mL ⁻¹] ^[f]	η [cP] ^[g]	κ [mS cm ⁻¹] ^[h]
1	$[C_1\text{mim}][\text{CF}_3\text{BF}_3]$				15	202	1.40	27	15.5
2	$[C_2\text{mim}][\text{CF}_3\text{BF}_3]$	-117	-80		-20	246	1.35	26	14.8
3	$[C_3\text{mim}][\text{CF}_3\text{BF}_3]$	-113	-63		-21	272	1.31	43	8.5
4	$[C_4\text{mim}][\text{CF}_3\text{BF}_3]$	-108				238	1.27	49	5.9
5	$[C_6\text{mim}][\text{CF}_3\text{BF}_3]$	-100				197	1.22	77	2.8
6	$[C_2\text{Omim}][\text{CF}_3\text{BF}_3]$				17	211	1.41	55	6.5
7	$[C_3\text{Omim}][\text{CF}_3\text{BF}_3]$	-99	-53		2	225	1.36	43	6.9
8	$[C_5\text{O}_2\text{mim}][\text{CF}_3\text{BF}_3]$	-87				238	1.31	62	3.4
9	$[C_1\text{mim}][\text{C}_2\text{F}_5\text{BF}_3]$				27	290	1.47	33	11.7
10	$[C_2\text{mim}][\text{C}_2\text{F}_5\text{BF}_3]$				1	305	1.42	27	12
11	$[C_3\text{mim}][\text{C}_2\text{F}_5\text{BF}_3]$	-111	-60		-42	312	1.38	35	7.5
12	$[C_4\text{mim}][\text{C}_2\text{F}_5\text{BF}_3]$	-106	-64		-42	309	1.34	41	5.5
13	$[C_6\text{mim}][\text{C}_2\text{F}_5\text{BF}_3]$	-100	-71		-10	306	1.28	59	2.7
14	$[C_2\text{Omim}][\text{C}_2\text{F}_5\text{BF}_3]$	-98	-48		-21	274	1.46	47	6
15	$[C_3\text{Omim}][\text{C}_2\text{F}_5\text{BF}_3]$	-98	-42		-9	288	1.42	38	6.1
16	$[C_5\text{O}_2\text{mim}][\text{C}_2\text{F}_5\text{BF}_3]$	-90				293	1.37	51	3.4
17	$[C_1\text{mim}][n\text{C}_3\text{F}_7\text{BF}_3]$			-8	11	279	1.55	47	7.3
18	$[C_2\text{mim}][n\text{C}_3\text{F}_7\text{BF}_3]$			-13	8	304	1.49	32	8.6
19	$[C_3\text{mim}][n\text{C}_3\text{F}_7\text{BF}_3]$				-5	298	1.44	44	5.3
20	$[C_1\text{mim}][n\text{C}_4\text{F}_9\text{BF}_3]$			16	35	275			
21	$[C_2\text{mim}][n\text{C}_4\text{F}_9\text{BF}_3]$				-4	277	1.55	38	5.2
22	$[C_3\text{mim}][n\text{C}_4\text{F}_9\text{BF}_3]$			-119	-12	305	1.48	59	3.5
23	$[C_2\text{mim}][\text{BF}_4]^{[i]}$	-93	-60		15	420	1.28	42	13.6
24	$[C_3\text{mim}][\text{BF}_4]^{[j]}$	-88	-38		-17	435	1.24	103	5.9
25	$[C_4\text{mim}][\text{BF}_4]^{[j]}$	-85				435	1.21	180	3.5
26	$[C_6\text{mim}][\text{BF}_4]$	-81 ^[k]				409	1.16	220	1.2

[a] Glass transition temperature determined by DSC on heating. [b] Crystallization temperature determined by DSC on heating. [c] Solid-solid transition temperature determined by DSC on heating. [d] Melting point determined by DSC on heating. [e] Decomposition temperature determined by TGA. [f] Density at 25°C. [g] Viscosity at 25°C. [h] Specific conductivity at 25°C. [i] The data agree with the literature.^[13,15b,c] [j] Literature data.^[15c] [k] -82°C .^[17]

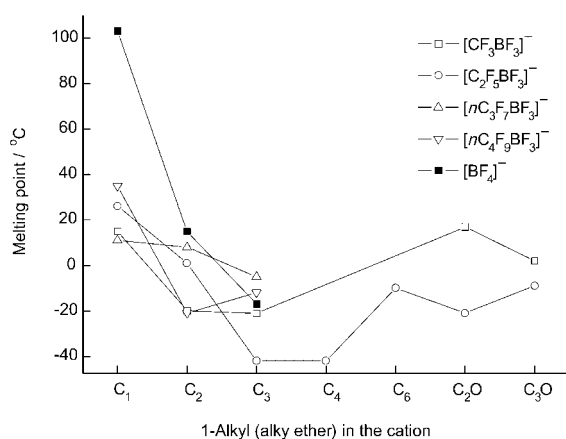


Figure 2. Melting point of various ionic liquid salts (observed); the melting point of the $[C_1mim][BF_4]$ was from literature.^[17]

ison. The T_m values of the $[R_FBF_3]^-$ -based salts fall between -42 and 35°C . With the exception of $[C_1mim][nC_4F_9BF_3]$ (T_m 35°C), all the $[R_FBF_3]^-$ -based salts are liquid at room temperature. For a given anion, the T_m values of the $[C_m\text{mim}][R_FBF_3]$ generally decreased as the 1-alkyl (C_m) chain length in the cation increased and reached a minimum at the alkyl = C_3 , and tended to increase with further lengthening the 1-alkyl (C_m) chain. This trend in T_m has been illustrated as a general feature of the 1,3-dialkylimidazolium salts, and is essentially related with the crystallinity of the salts.^[14,17,20,32] It was expected that replacing the 1-alkyl (C_m) in the cation with a more flexible alkyl ether (C_mO_n) group would result in a decrease in T_m ; however, an opposite trend was observed (Table 2, entry 3 vs 6, 11 vs 14, 12 vs 15). Considering the fact that the polarity is higher for an alkyl ether group than for an alkyl group, this unexpected result might be due to the polarity of the alkyl ether group, which dominates over its flexibility, and introducing a polar alkyl ether group into the imidazolium cations turns to increase ion-ion and van der Waals interactions in the salts, thus raising T_m .

Comparison of the T_m values of the $[R_FBF_3]^-$ -based salts with those of the $[BF_4]^-$ -based ones clearly shows the impact of the anion symmetry. For the same cation, the salts with lower symmetry $[R_FBF_3]^-$ generally exhibit a low melting point than those with higher symmetry $[BF_4]^-$. This difference is more significant for the salts with the high symmetry $[C_1mim]^+$ cation (Table 2, entries 1, 9, 17, 20 vs $[C_1mim][BF_4]$ (T_m 103°C)^[17] and $[C_1mim][PF_6]$ (T_m 89°C)^[32a]). These results suggest that packing efficiency of the salt could be disrupted by reducing the anion symmetry, thus lowering the melting point. However, as seen in Figure 2, there is still no clear relationship between the structure and chemical composition of these salts and their melting points.

Figure 3 shows the glass transition temperatures (T_g) of these new salts and the salts with $[BF_4]^-$. It is very interesting that the $[R_FBF_3]^-$ -based salts containing the shorter perfluoroalkyl chains ($R_F = \text{CF}_3, \text{C}_2\text{F}_5$) exhibited glass-forming ability at an extremely low temperature while all those containing the longer perfluoroalkyl chains ($R_F = n\text{C}_3\text{F}_7, n\text{C}_4\text{F}_9$)

did not under the same conditions. As shown in Figure 3, the trend for the T_g values is much more regular than that for the T_m values. For each anion, the T_g values of these

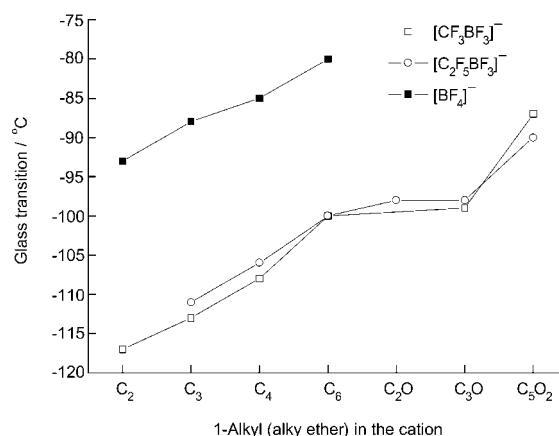


Figure 3. Glass transition temperature of various ionic liquids (observed).

salts generally increase progressively with increasing the length of the 1-alkyl (C_m) chain in the cation, perhaps owing to an additional energy required to reorient larger cations in the glassy state. As observed in the melting point, replacing the 1-alkyl (C_m) group in the cation with an isoelectronic or longer alkyl ether (C_mO_n) group resulted in an increase in T_g (Table 2, entry 4 vs 7, 5 vs 8, 11 vs 14, 12 vs 15, 13 vs 16). For the same cation, the T_g values of the $[CF_3BF_3]^-$ -based salts are almost the same as those of the $[C_2F_5BF_3]^-$ -based ones; however, the T_g values of the $[R_FBF_3]^-$ -based salts ($R_F = \text{CF}_3, \text{C}_2\text{F}_5$) are obviously lower than those of the corresponding $[BF_4]^-$ -based ones presumably as a consequence of a better charge distribution in the $[R_FBF_3]^-$. In addition, the extremely low T_g values of the $[R_FBF_3]^-$ -based salts (ranging from -87 to -117°C) reflect that the ions in these salts have a high mobility, which may partly account for their low viscosities (see below).

Thermogravimetric analysis: The thermal stability of the salts in the present study was determined by TGA. Figure 4

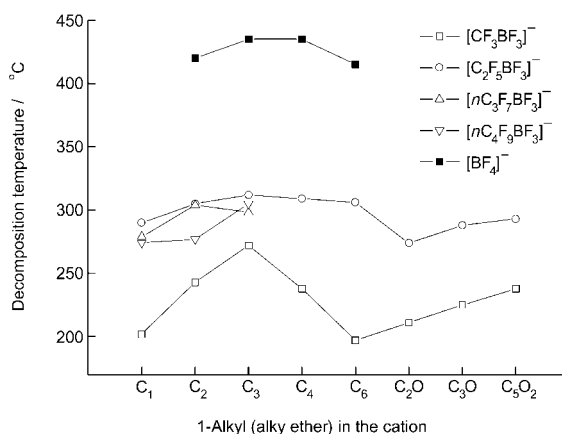


Figure 4. Thermal stability of various ionic liquids.

shows the decomposition temperatures (T_d) of the $[\text{R}_F\text{BF}_3]^-$ and $[\text{BF}_4]^-$ -based salts. The T_d values for the $[\text{CF}_3\text{BF}_3]^-$ -based salts are in the range of 197–272 °C, and 274–312 °C for the other $[\text{R}_F\text{BF}_3]^-$ -based salts ($\text{R}_F = \text{C}_2\text{F}_5$, $n\text{C}_3\text{F}_7$, $n\text{C}_4\text{F}_9$), and 409–435 °C for the $[\text{BF}_4]^-$ -based salts. Apparently, the salts with the inorganic $[\text{BF}_4]^-$ are much more stable by about 100 °C than those with the organic $[\text{R}_F\text{BF}_3]^-$, and the thermal stability of these salts generally increases in the order $[\text{CF}_3\text{BF}_3]^- < [\text{C}_2\text{F}_5\text{BF}_3]^-$, $[\text{nC}_3\text{F}_7\text{BF}_3]^-$, $[\text{nC}_4\text{F}_9\text{BF}_3]^- \ll [\text{BF}_4]^-$. These results indicate that the anion has a significant impact on the thermal stability of these imidazolium salts. To gain an insight into the impact of the anion on the thermal stability, the thermogravimetric traces of five $[\text{C}_2\text{mim}]^+$ -based salts with different anions as examples are displayed in Figure 5. As shown in Figure 5, the decomposition behav-

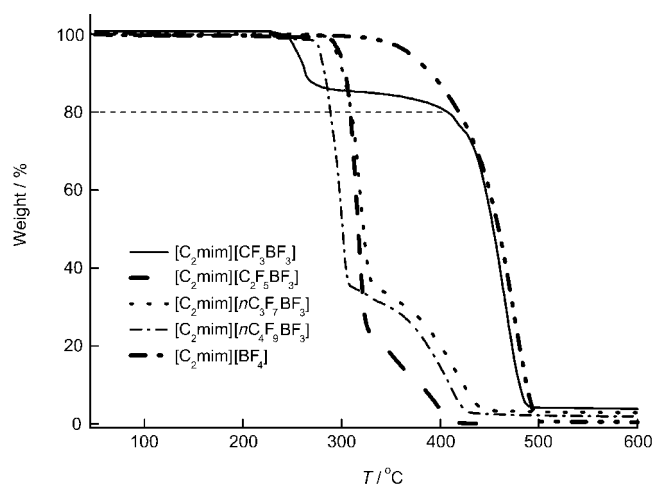


Figure 5. TGA traces of the salts $[\text{C}_2\text{mim}][\text{R}_F\text{BF}_3]$ ($\text{R}_F = \text{CF}_3$, C_2F_5 , $n\text{C}_3\text{F}_7$, $n\text{C}_4\text{F}_9$) and $[\text{C}_2\text{mim}][\text{BF}_4]$.

ior of the $[\text{C}_2\text{mim}][\text{R}_F\text{BF}_3]$ ($\text{R}_F = \text{CF}_3$, C_2F_5 , $n\text{C}_3\text{F}_7$, $n\text{C}_4\text{F}_9$) is significantly different from that of the $[\text{C}_2\text{mim}][\text{BF}_4]$. The decomposition rate of the $[\text{C}_2\text{mim}][\text{BF}_4]$ almost remained constant during the pyrolysis (ca. 400–500 °C). However, the decomposition rate of the $[\text{C}_2\text{mim}][\text{CF}_3\text{BF}_3]$ varied significantly during the pyrolysis, it became rapid from about 240 °C and turned slow after reaching ≈ 270 °C, and became almost the same as that of the $[\text{C}_2\text{mim}][\text{BF}_4]$ from ≈ 410 °C. The weight loss percentage of the $[\text{C}_2\text{mim}][\text{CF}_3\text{BF}_3]$ from ≈ 240 to 270 °C was $\approx 20\%$ in correspondence to elimination of a CF_2 moiety from the $[\text{C}_2\text{mim}][\text{CF}_3\text{BF}_3]$, likely $[\text{CF}_3\text{BF}_3]^- \rightarrow [\text{BF}_4]^- + \text{other products}$ (formed from CF_2 carbene), which was also supported by its subsequent decomposition behavior above 410 °C (see Figure 5). The decomposition of the $[\text{R}_F\text{BF}_3]^-$ -based salts ($\text{R}_F = \text{C}_2\text{F}_5$, $n\text{C}_3\text{F}_7$, $n\text{C}_4\text{F}_9$) also varied during the process, and exhibited a very complex mode as illustrated in Figure 5. These results suggest that the low thermal stability of the salts with $[\text{R}_F\text{BF}_3]^-$ may be caused by the pyrolysis of $[\text{R}_F\text{BF}_3]^-$ at a low temperature, and the acidity of the H(2) in the imidazolium ring might have a contribution to this process.^[19] However, for a constant anion, it appears that the variation in the imidazolium cation has less effect on the stability of the corresponding salts as shown in Figure 4.

Density: Figure 6 displays the densities of the liquid salts (the new ILs $[\text{C}_m\text{O}_n\text{mim}][\text{R}_F\text{BF}_3]$ and $[\text{C}_m\text{O}_n\text{mim}][\text{BF}_4]$, and the $[\text{C}_m\text{mim}][\text{BF}_4]$) at 25 °C. The density is in the range

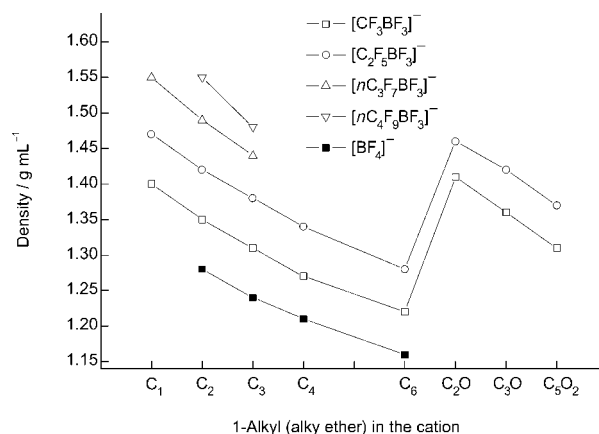


Figure 6. Density of various liquid salts at 25 °C.

of 1.16–1.55 g mL^{-1} . With a constant anion, the density decreased with the length of 1-alkyl (alkyl ether) chain in the cation increased, for example, keeping the $[\text{CF}_3\text{BF}_3]^-$ constant (Table 2, entries 1–8), $1 > 2 > 3 > 4 > 5$ ($\text{C}_1 > \text{C}_2 > \text{C}_3 > \text{C}_4 > \text{C}_6$) and $6 > 7 > 8$ ($\text{C}_1\text{O} > \text{C}_3\text{O} > \text{C}_5\text{O}_2$). The density of the $[\text{C}_m\text{O}_n\text{mim}]^+$ -based ILs is a little higher than those of the similar $[\text{C}_m\text{mim}]^+$ -based ones, for example, $6 > 3$ ($\text{C}_2\text{O} > \text{C}_3$) and $7 > 4$ ($\text{C}_3\text{O} > \text{C}_4$). These trends are consistent with the reported observations in other ILs with imidazolium cations.^[1c,4c,30] On the other hand, with a constant cation, the density increased with increasing the bulkiness of the anion in the order $[\text{BF}_4]^- < [\text{CF}_3\text{BF}_3]^- < [\text{C}_2\text{F}_5\text{BF}_3]^- < [\text{nC}_3\text{F}_7\text{BF}_3]^- < [\text{nC}_4\text{F}_9\text{BF}_3]^-$. As shown in Figure 6, it seems that the density of these salts linearly decreased as the length of 1-alkyl (C_m) or 1-alkyl ether (C_mO_n) chain in the cation increased and linearly increased as the number of fluorine atoms in the $[\text{C}_n\text{F}_{2n+1}\text{BF}_3]^-$ ($n = 0–4$) increased. In the $[\text{C}_m\text{mim}][\text{C}_n\text{F}_{2n+1}\text{BF}_3]$ series ($m = 1–4$ and 6, $n = 0–4$) (nineteen liquid salts), such a linear relationship was observed as follows: d (g mL^{-1}) = $1.36 - 0.037m + 0.064n$ ($r = 0.993$). These results indicate that the densities of these ionic liquids can be fine-tuned with slight structural changes in the cation and anion.

Viscosity: The viscosity of an ionic liquid is essentially determined by their tendency to form hydrogen bonds and by the strength of van der Waals interactions (dispersion and repulsion), being strongly dependent on the anion type.^[14] For the imidazolium ILs, longer alkyl chains on the cation result in an increase in viscosity due to stronger van der Waals interactions whereas delocalization of the charge over the anion seems to favor lower viscosity by weakening hydrogen bonding with the cation.^[8–14,18,20] In addition, an anion combined a good charge distribution and a flat shape (e.g. $[\text{F}(\text{HF})_{2.3}]^-$,^[7] $[\text{N}(\text{CN})_2]^-$,^[9,10] and $[\text{C}(\text{CN})_3]^-$ ^[10,11]) or an irregular shape (e.g., $[\text{Al}_2\text{Cl}_7]^-$,^[8] $[(\text{CF}_3\text{SO}_2)(\text{CF}_3\text{CO})\text{N}]^-$,^[12] and $[(\text{CF}_3\text{SO}_2)_2\text{N}]^-$ ^[13,14]) tends to form low-viscous ILs,

while that with high symmetry (e.g., BF_4^- ,^[13,15c,18,20] PF_6^- ,^[18,20,30,32b] AsF_6^- ,^[16a] SbF_6^- ,^[16a] and TaF_6^- ^[16a]) usually produces high-viscous and/or high-melting salts in spite of its weakly coordinating ability.

Figure 7 shows the viscosities (η) of the liquid salts (the new $[\text{C}_m\text{mim}][\text{R}_F\text{BF}_3]$ and $[\text{C}_m\text{O}_n\text{mim}][\text{R}_F\text{BF}_3]$, and the reported $[\text{C}_m\text{mim}][\text{BF}_4]$) at 25 °C. For all the $[\text{C}_m\text{mim}]^+$ -based ILs with the same anion, the viscosities generally increased as the 1-alkyl (C_m) chain increased, which is essentially attributed to the increase of van der Waals interactions. This trend agrees with those reported previously.^[14,32b] The influence of replacing the 1-alkyl (C_m) group with a similar alkyl ether (C_mO_n) group on the viscosity is highly dependent on their structures. For instance, replacing the 1- C_4 group with a C_3O_1 group, or the 1- C_6 group with a longer C_5O_2 group, resulted in a decrease in viscosity (Table 2, entry 4 vs 7, 5 vs 8, 12 vs 15, 13 vs 16), whereas a viscosity increase was observed for replacing the 1- C_3 group with a C_2O_1 group (Table 2, entry 3 vs 6, 11 vs 14). Although the exact reasons for the effect of the alkyl ether group on the viscosity of these salts are not well understood, it is believed to be associated with the competing influences of ion-ion and van der Waals interactions and freedoms of the ions in these salts, as discussed in T_m trend previously.

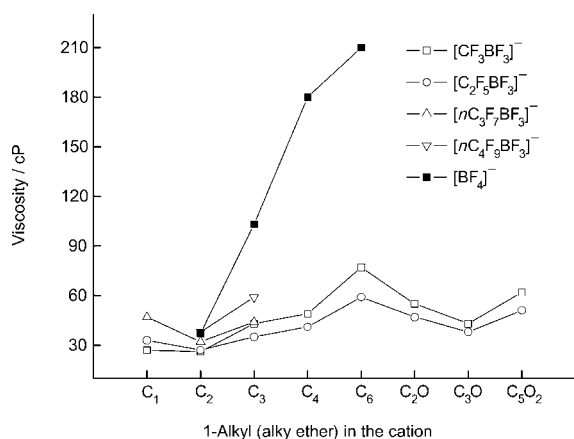


Figure 7. Viscosity of various liquid salts at 25 °C.

Comparing the viscosities of the $[\text{R}_F\text{BF}_3]^-$ -based ILs with those of the $[\text{BF}_4]^-$ -based ones immediately displays the impact of the anion. As seen in Figure 7, the viscosities of all the $[\text{R}_F\text{BF}_3]^-$ -based ILs ($\text{R}_F = \text{CF}_3$, C_2F_5 , $n\text{C}_3\text{F}_7$, $n\text{C}_4\text{F}_9$) at 25 °C are in the range 26–77 cP, which are comparable to those of the corresponding $[(\text{CF}_3\text{SO}_2)_2\text{N}]^-$ -based ones (34–83 cP at 20 °C),^[14] and obviously lower than those of the corresponding $[\text{BF}_4]^-$ -based ones (43–220 cP at 25 °C, Table 2),^[15c,20] and significantly lower than those of the corresponding $[\text{PF}_6]^-$ -based ones (148–363 cP at 30 °C^[30]). This difference is more noticeable for the ILs with the large cations (Table 2, entries 3, 11, 19, 22 vs 24; entries 5, 13 vs 26). These results indicate that 1) replacing one fluorine atom in the $[\text{BF}_4]^-$ with a strongly electron-withdrawing perfluoroalkyl (R_F) group makes the negative charge more delocalized, thus weakening the electrostatic interactions (including

possible hydrogen bonding) between the cation and anion, 2) the decrease of the electrostatic interactions prevail over the increase of van der Waals attractions (the anion size increased) because of the low polarizability of fluorine atom, and 3) the relatively low symmetry of the $[\text{R}_F\text{BF}_3]^-$ may reduce the ion interactions through destabilizing the crystal lattice of the salts. In the $[\text{R}_F\text{BF}_3]^-$ series ($\text{R}_F = \text{CF}_3$, C_2F_5 , $n\text{C}_3\text{F}_7$, $n\text{C}_4\text{F}_9$), the ILs with the larger $[\text{R}_F\text{BF}_3]^-$ ($\text{R}_F = n\text{C}_3\text{F}_7$, $n\text{C}_4\text{F}_9$) afforded a higher viscosity than those with the smaller $[\text{R}_F\text{BF}_3]^-$ ($\text{R}_F = \text{CF}_3$, C_2F_5), suggesting that a very large anion is unfavorable to produce low-viscous ILs in spite of its good charge delocalization. Interestingly, apart from the $[\text{C}_1\text{mim}][\text{CF}_3\text{BF}_3]$ and $[\text{C}_2\text{mim}][\text{CF}_3\text{BF}_3]$, all the ILs with the larger $[\text{C}_2\text{F}_5\text{BF}_3]^-$ showed a little lower viscosity than those with the smaller $[\text{CF}_3\text{BF}_3]^-$, which is probably due to a better charge delocalization in the former anion. Among these new ILs, three of them exhibit the lowest viscosities, 26 cP for $[\text{C}_2\text{mim}][\text{CF}_3\text{BF}_3]$ and 27 cP for $[\text{C}_1\text{mim}][\text{CF}_3\text{BF}_3]$ and $[\text{C}_2\text{mim}][\text{C}_2\text{F}_5\text{BF}_3]$ at 25 °C, all of which are a bit lower than that for the hydrophobic representative $[\text{C}_2\text{mim}][(\text{CF}_3\text{SO}_2)_2\text{N}]$ (28 cP at 25 °C).^[13] All the above results suggest that, in search of low-viscous ILs, one must not only focus on weakly coordinating ability of the anion, the shape (symmetry) and size of the anion should keep in mind.

Conductivity: Figure 8 shows the specific conductivities (κ) of the liquid salts (the new $[\text{C}_m\text{mim}][\text{R}_F\text{BF}_3]$ and $[\text{C}_m\text{O}_n\text{mim}][\text{R}_F\text{BF}_3]$, and the reported $[\text{C}_m\text{mim}][\text{BF}_4]$) at 25 °C. In the $[\text{R}_F\text{BF}_3]^-$ -based series ($\text{R}_F = \text{CF}_3$, C_2F_5 , $n\text{C}_3\text{F}_7$, $n\text{C}_4\text{F}_9$), the conductivities generally decreased as the formula weight of the imidazolium ($[\text{C}_m\text{mim}]^+$ and $[\text{C}_m\text{O}_n\text{mim}]^+$) cation and $[\text{R}_F\text{BF}_3]^-$ anion increased, namely, the extension of the 1-alkyl(alkyl ether) chain in the cation and the perfluoroalkyl (R_F) chain in the $[\text{R}_F\text{BF}_3]^-$.

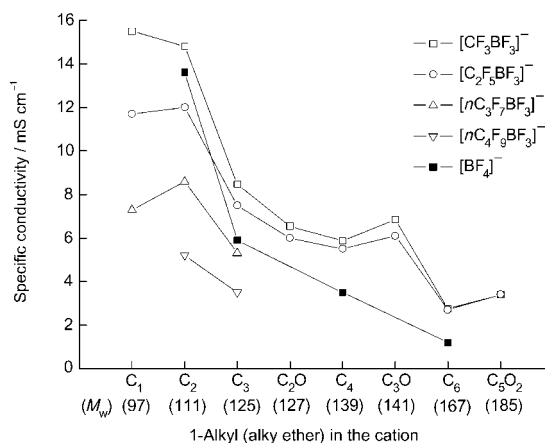


Figure 8. Specific conductivity of various liquid salts at 25 °C; the data in parentheses is formula weight (M_w) of the cations $[\text{C}_m\text{mim}]^+$ and $[\text{C}_m\text{O}_n\text{mim}]^+$.

The conductivities of the ILs are mainly governed by their viscosities, molecular weight, densities, and ion sizes of the ILs.^[14] The viscosity determines the ion mobility while the latter three factors determine the number of carrier

ions. Comparing the conductivities of the $[\text{R}_F\text{BF}_3]^-$ -based ILs with those of the $[\text{BF}_4]^-$ -based ones clearly illustrates the interplay among these factors. As shown in the previous section, all the $[\text{R}_F\text{BF}_3]^-$ -based ILs exhibit a lower viscosity than the corresponding $[\text{BF}_4]^-$ -based one (see Figure 7); however, the $[\text{R}_F\text{BF}_3]^-$ -based ILs with shorter R_F chains ($\text{R}_F = \text{CF}_3, \text{C}_2\text{F}_5$) exhibit a higher or comparable conductivity than the $[\text{BF}_4]^-$ -based one; this indicates the viscosity decrease dominates over the increases of molecular weight, density, and anion size, whereas those with longer R_F chains ($\text{R}_F = n\text{C}_3\text{F}_7, n\text{C}_4\text{F}_9$) afford a lower conductivity than the corresponding $[\text{BF}_4]^-$ -based one, showing the viscosity decrease overcompensates for the increases of the latter three factors (see Figure 8). Furthermore, the conductivity of the $[\text{R}_F\text{BF}_3]^-$ -based ILs with short R_F chains ($\text{R}_F = \text{CF}_3, \text{C}_2\text{F}_5$) is apparently higher than that of the $[(\text{CF}_3\text{SO}_2)_2\text{N}]^-$ -based one with the same cation in spite of their similar viscosities,^[13,14] further reinforcing that an anion with a large formula weight and size is unsuitable for producing highly conductive ILs. Among these new hydrophobic ILs, two salts, $[\text{C}_1\text{mim}][\text{CF}_3\text{BF}_3]$ and $[\text{C}_2\text{mim}][\text{CF}_3\text{BF}_3]$, have the lowest viscosities (25–26 cP at 25 °C) combined small molecular weight and moderate ion sizes, thus resulting in the highest conductivities, 15.5 mS cm^{-1} for the former and 14.6 mS cm^{-1} for the latter. To our best knowledge, these two salts have the highest conductivities among the hydrophobic ILs reported,^[4a,14] which are even a little higher than a conventional electrolyte solutions, 1 mol dm^{-3} $[(\text{C}_2\text{H}_5)_3\text{CH}_3\text{N}][\text{BF}_4]$ in propylene carbonate (13 mS cm^{-1}), for double-layer capacitor.^[34] From these results, we could conclude that, when seeking for highly conductive ILs, investigators should take into account not only the viscosity but also the other factors as described above, especially the molecular weight.

It has been reported recently that the empirical Walden rule founded in a wide range of aqueous electrolyte solution, that is, the product of $\Lambda\eta$ remains constant (Λ is the equivalent conductivity of the electrolyte and η the viscosity),^[35] is valid for many ILs.^[8c,10] Assuming that the ions in each liquid salt in this study are dissociated completely, this allows the equivalent conductivity (Λ) of these ILs to be calculated by the equation $\Lambda = \kappa M/d$, wherein M , κ , and d represent the specific conductivity, formula weight, and density of the corresponding ILs, respectively. Figure 9 displays the plot of the calculated equivalent conductivity (Λ) of twenty one $[\text{R}_F\text{BF}_3]^-$ -based liquid salts (see Table 2, entries 1–19, 21 and 22) as a function of the reciprocal of the viscosity (η^{-1}) at 25 °C. A nearly linear relationship between the calculated equivalent conductivity and the reciprocal of the viscosity was observed in Figure 9 ($r = 0.953$). This result indicates that the dissociation extents in these ILs are very close and should be very high because of the weakly coordinating ability of the $[\text{R}_F\text{BF}_3]^-$, and Walden rule may be applicable for these new ILs. To further verify whether these ILs obey Walden rule, the product of $\Lambda\eta$ for each salt in a wide temperature range must be studied.

Electrochemical stability: The electrochemical stability of nine salts based on the $[\text{C}_2\text{mim}]^+$ and $[\text{C}_4\text{mim}]^+$ with various anions including $[\text{R}_F\text{BF}_3]^-$ ($\text{R}_F = \text{CF}_3, \text{C}_2\text{F}_5, n\text{C}_3\text{F}_7, n\text{C}_4\text{F}_9$),

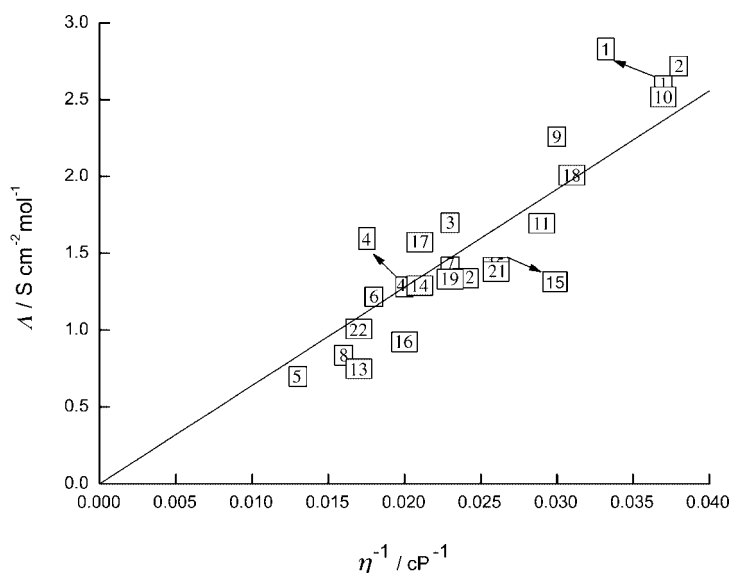


Figure 9. A plot of the equivalent conductivity (Λ) against the reciprocal of the viscosity (η^{-1}) for 21 liquid salts based on the $[\text{R}_F\text{BF}_3]^-$ ($\text{R}_F = \text{CF}_3, \text{C}_2\text{F}_5, n\text{C}_3\text{F}_7, n\text{C}_4\text{F}_9$), where the number is consistent with entries 1–22 in Table 2.

$[\text{BF}_4]^-$ and $[(\text{CF}_3\text{SO}_2)_2\text{N}]^-$ was comparatively studied by linear sweep voltammetry (LSV) on a glassy carbon electrode. Figure 10 shows the LSV curves of these salts determined in the first scan under the same measurement conditions, where the potential is referenced to ferrocene (Fc)/ferrocenium (Fc^+) redox system in each salt, as the potential of the Fc/Fc^+ system is little affected by nonaqueous solvents.^[36] As shown in Figure 10, all these nine salts almost show an equivalent electrochemical window. This result is consistent with recent literatures,^[15c,29a] where the $[\text{C}_m\text{mim}]^+$ -based salts ($m = 2–4$) with the $[\text{BF}_4]^-$ and $[\text{C}_2\text{F}_5\text{BF}_3]^-$ showed an equivalent electrochemical window on a Pt elec-

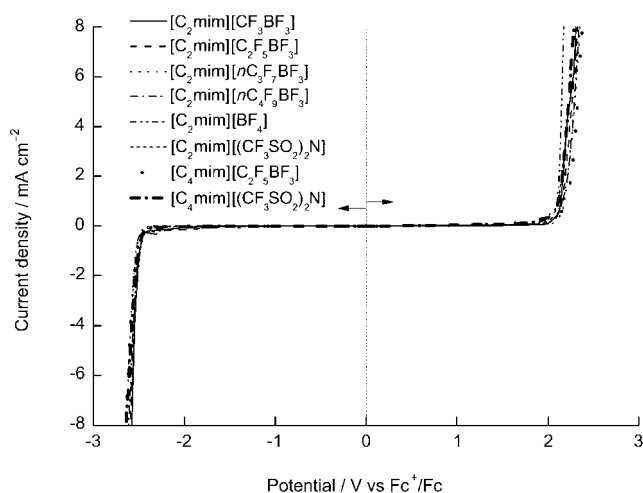


Figure 10. Linear sweep voltammogram of various ionic liquids on a glassy carbon electrode (surface area: $7.85 \times 10^{-3} \text{ cm}^2$) in the first scan; scan rate: 50 mV s^{-1} ; counter electrode: Pt wire; potential (V) was referred to ferrocene (Fc)/ferrocenium (Fc^+) redox couple in each salt; water content: ca. 200 ppm in the $[\text{C}_2\text{mim}][\text{BF}_4]^-$ and < 50 ppm in the other salts.

trode, and both the oxidation and reduction potentials were not affected by the alkyl chain length in the cation or by replacing the $[\text{BF}_4]^-$ with a $[\text{C}_2\text{F}_5\text{BF}_3]^-$. However, the quaternary ammonium salts of these anions are more significantly resistant against the reduction and oxidation than the corresponding 1,3-dialkylimidazolium salts, and show much larger electrochemical windows than the latter.^[37] These results strongly indicate that not only the cathodic but also the anodic decomposition of the salts in this study are limited by the 1,3-dialkylimidazolium cations, such as $[\text{C}_2\text{mim}]^+$ and $[\text{C}_4\text{mim}]^+$. Therefore, it seems reasonable that the anions, such as the $[\text{R}_F\text{BF}_3]^-$, $[\text{BF}_4]^-$ and $[(\text{CF}_3\text{SO}_2)_2\text{N}]^-$, are more stable against the reduction and oxidation than 1,3-dialkylimidazolium cations.

The respective cathodic and anodic limits and electrochemical windows are given in Table 3, where the limit was set as the potential at which the current density reached 1 mA cm^{-2} . As seen in Table 3, the electrochemical window values for these salts are very close, and obviously larger than those for the highly conductive salts with $[\text{N}(\text{CN})_2]^-$,^[9a,10] and $[\text{C}(\text{CN})_3]^-$.^[10,11] However, one may note that the electrochemical window value for the $[\text{C}_2\text{mim}][\text{BF}_4]$ (4.55 V) is a little narrower than those for the other salts (Table 3). This may be caused by the presence of relatively high contents of water and HF in the $[\text{C}_2\text{mim}][\text{BF}_4]$ (ca. 200 ppm water and ca. 240 ppm F^- (HF)), because it has been identified recently that a bit increase in water content in ILs dramatically shortens the electrochemical windows of ILs.^[38] In addition, it should be noted that the electrochemical window of the ILs is highly dependent on the type of electrode used.^[39] For example, for the same salt $[\text{C}_4\text{mim}][\text{BF}_4]$, the electrochemical window value measured on a glassy carbon electrode in this study is 4.68 V, which is larger than that determined on a Pt electrode ($< 4.6 \text{ V}$ ^[29a,38,39]); however, much larger electrochemical windows for the $[\text{C}_4\text{mim}][\text{BF}_4]$ were also reported on glassy carbon and tungsten electrodes (5.45 V for the former and 6.10 V for the latter) in the literature,^[39] due to the potential hysteresis which was possibly caused by electrochemical decomposition of electroactive impurities and adsorption of the products on the electrode, as explained by the authors.^[39]

Conclusion

A series of chemically and electrochemically stable, hydrophobic ionic liquids consisting of $[\text{R}_F\text{BF}_3]^-$ anion with 1-alkyl(alkyl ether)-3-methylimidazolium cation were synthesized and characterized. The most prominent features of these new ILs are their low melting points and low viscosities (26–77 cP at 25 °C) due to relatively low symmetry and good charge distribution in the $[\text{R}_F\text{BF}_3]^-$. Some of them with small molecular weight also exhibit high conductivities that could be comparable to conventional electrolyte solutions. All these desired properties may support them as new solvents for organic and biocatalytic reactions, and as potential electrolytes for electrochemical devices.

Experimental Section

General: The following materials were prepared and purified according to the reported procedure: potassium perfluoroalkyltrifluoroborate $\text{K}[\text{R}_F\text{BF}_3]$ ($\text{R}_F = \text{CF}_3$, C_2F_5 , $n\text{C}_3\text{F}_7$, $n\text{C}_4\text{F}_9$);^[23–26] 1,3-dimethylimidazolium iodide ($[\text{C}_1\text{mim}]\text{I}$), 1-ethyl-3-methylimidazolium chloride ($[\text{C}_2\text{mim}]\text{Cl}$), 1-methyl-3-*n*-propylimidazolium chloride ($[\text{C}_3\text{mim}]\text{Cl}$), 1-ethyl-3-*n*-butylimidazolium chloride ($[\text{C}_4\text{mim}]\text{Cl}$), 1-ethyl-3-*n*-hexylimidazolium chloride ($[\text{C}_6\text{mim}]\text{Cl}$), 1-methoxymethyl-3-methylimidazolium chloride ($[\text{C}_2\text{Omim}]\text{Cl}$), 1-(2-methoxyethyl)-3-methylimidazolium bromide ($[\text{C}_3\text{Omim}]\text{Br}$), 1-[2-(2-methoxyethoxy)ethyl]-3-methylimidazolium bromide ($[\text{C}_5\text{O}_2\text{mim}]\text{Br}$).^[14,17,18,30] The imidazolium halide salts were purified by recrystallization from anhydrous acetonitrile/ethyl acetate under nitrogen atmosphere. The salts $[\text{C}_2\text{mim}][\text{BF}_4]$,^[15a] $[\text{C}_4\text{mim}][\text{BF}_4]$,^[17] $[\text{C}_6\text{mim}][\text{BF}_4]$ ^[17] and $[\text{C}_2\text{mim}][(\text{CF}_3\text{SO}_2)_2\text{N}]$ ^[14] were synthesized according to the literature.

NMR spectra were obtained using a JEOL JNM AL400 spectrometer (^1H at 399.65 MHz, ^{19}F at 376.05 MHz, and ^{11}B at 128.15 MHz), and $[\text{D}_6]\text{acetone}$ was used as solvent. Chemical shift values are reported in ppm with respect to TMS internal reference for ^1H , and external references CCl_3F in $[\text{D}_6]\text{acetone}$ for ^{19}F and $\text{BF}_3 \cdot \text{Et}_2\text{O}$ in CDCl_3 for ^{11}B . FAB-MS (FAB⁺ and FAB⁻) were measured on a JEOL DX303 spectrometer. Element analysis (C, H, and N) was performed at the Sumika Chemical Analysis Centre of Osaka.

Water content: The water content in the ILs was detected by Karl-Fischer titration (Mitsubishi Chem., model CA-07). With the exception of $[\text{C}_2\text{mim}][\text{BF}_4]$ (water content: ca. 200 ppm), all the salts prepared in the present study contained less than 50 ppm of water after vacuum drying at 70–100 °C for 24 h.

Impurity measurements: F^- (HF) content in the salts was determined by ion chromatography at the Sumika Chemical Analysis Centre of Osaka. The F^- (HF) content was < 5 ppm in the $[\text{R}_F\text{BF}_3]^-$ -based salts and ca. 240 ppm in the $[\text{C}_2\text{mim}][\text{BF}_4]$. The amount of residual halide (Cl^- , Br^- , or I^-) and potassium ions in the ILs was approximately estimated by a fluorescence X-ray spectrometer (JEOL, model JSX-3201), and was revealed to be less than 50 ppm.

Phase-transition analysis: The calorimetric measurements were performed with a differential scanning calorimeter (Perkin–Elmer Pyris 1 DSC equipped with a liquid nitrogen cryostatic cooling). An average sample weight of 5–10 mg was sealed in an aluminum pan and quenched, initially to -150 °C, and then heated and cooled between -150 °C and a predetermined temperature at a rate of 10 °C min^{-1} under a flow of helium. The glass transition temperature (T_g , onset of the heat capacity change), crystallization temperature (T_c , onset of the exother-

Table 3. Electrochemical windows for various ionic liquids determined on a glassy carbon electrode.

Salts	Cathodic limit ^[a] [V]	Anodic limit ^[a] [V]	Electrochemical window [V]
$[\text{C}_2\text{mim}][\text{CF}_3\text{BF}_3]$	−2.49	2.14	4.63
$[\text{C}_2\text{mim}][\text{C}_2\text{F}_5\text{BF}_3]$	−2.50	2.15	4.65
$[\text{C}_2\text{mim}][n\text{C}_3\text{F}_7\text{BF}_3]$	−2.53	2.18	4.71
$[\text{C}_2\text{mim}][n\text{C}_4\text{F}_9\text{BF}_3]$	−2.51	2.16	4.67
$[\text{C}_2\text{mim}][\text{BF}_4]$	−2.45	2.10	4.55
$[\text{C}_2\text{mim}][(\text{CF}_3\text{SO}_2)_2\text{N}]$	−2.48	2.11	4.59
$[\text{C}_4\text{mim}][\text{C}_2\text{F}_5\text{BF}_3]$	−2.52	2.21	4.73
$[\text{C}_4\text{mim}][\text{BF}_4]$	−2.55	2.13	4.68
$[\text{C}_4\text{mim}][(\text{CF}_3\text{SO}_2)_2\text{N}]$	−2.50	2.12	4.62

[a] The limit was set as the potential at which the current density reached 1 mA cm^{-2} ; all potentials (V) vs ferrocene (Fc)/ferrocenium (Fc^+).

mic peak), solid–solid transition temperature (T_{s-s} , onset of the endothermic peak), melting point (T_m , onset of the endothermic peak) were determined on heating in the second heating-cooling cycle.

Thermal gravimetric analysis (TGA): The TGA was performed on a thermal analysis system (Seiko Instruments, TG/DTA 6200). An average sample weight of 5 mg was placed in a platinum pan and heated at $10^\circ\text{C min}^{-1}$ from ca. 40 to 600°C under a flow of nitrogen. The onset of decomposition was defined as the decomposition temperature (T_d).

Viscosity: The viscosity was measured with a viscometer (Brookfield, model DV-III+) using 0.6 mL sample at 25°C .

Density: The density of the liquid salts was approximately determined by measuring the weight of 1.0 mL of the salt three times at 25°C .

Specific conductivity: The ionic conductivity (κ) of the neat ILs was measured by a conductivity meter (Radiometer Analytical, model CDM230) in a sealed conductivity cell at 25°C .

Electrochemical stability: Linear sweep voltammetry (LSV) was performed using an automatic polarization system (ALS, model 600) in an argon-filled glove box (O_2 and water <5 ppm), by using a 5 mL beaker-type three-electrode cell equipped with a glassy carbon electrode (surface area: $7.85 \times 10^{-3} \text{ cm}^2$), a Pt wire counter electrode, and an I_3^-/I^- reference electrode consisting of Pt wire/ $0.015 \text{ mol dm}^{-3} \text{ I}_2 + 0.060 \text{ mol dm}^{-3} [(\text{C}_2\text{H}_5)_3\text{N}]\text{I}$ in the $[\text{C}_2\text{mim}][(\text{CF}_3\text{SO}_2)_2\text{N}]$. The potential was referenced to ferrocene (Fc)/ferrocenium (Fc^+) redox couple in each salt. The values for the cathodic and anodic limits and the electrochemical windows of the salts were undertaken in the first scan. The limit was arbitrarily set as the potential at which the current density reached 1 mA cm^{-2} .

Synthesis of ionic liquids: The salts $[\text{C}_m\text{mim}][\text{R}_f\text{BF}_3]$ and $[\text{C}_m\text{Omim}][\text{R}_f\text{BF}_3]$ were synthesized by metathesis reactions of the corresponding 1-alkyl-3-methylimidazolium halide with a little excess of $\text{K}[\text{R}_f\text{BF}_3]$ (1.05 equiv). In a typical reaction, to a stirred solution of $[\text{C}_2\text{mim}]\text{Cl}$ (4.40 g, 30 mmol) in water (15 mL) was added $\text{K}[\text{CF}_3\text{BF}_3]$ (5.45 g, 31 mmol) at room temperature. The mixture was stirred for an additional 30 min. The bottom layer was separated, dissolved in dichloromethane (15 mL), and washed with water twice (2×5 mL). After evaporation, the liquid obtained was dried at 70°C and 0.02 Torr for 24 h, affording the $[\text{C}_2\text{mim}][\text{CF}_3\text{BF}_3]$ (6.32 g, 85%) as a colorless liquid (water content: 48 ppm). The others were similarly prepared in a 30 mmol scale.

1,3-Dimethylimidazolium trifluoromethyltrifluoroborate ($[\text{C}_2\text{mim}][\text{CF}_3\text{BF}_3]$): 75% yield, pale yellow liquid; $^1\text{H NMR}$: $\delta = 4.02$ (s, 2×3 H), 7.66 (s, 2H), 8.89 ppm (s, 1H); $^{19}\text{F NMR}$: $\delta = -74.8$ (q, $^2J(\text{B,F}) = 32.6$ Hz, 3F; CF_3), -155.2 ppm (q, $^1J(\text{B,F}) = 39.6$ Hz, 3F; BF_3); $^{11}\text{B NMR}$: $\delta = -0.47$ ppm (qq, $^1J(\text{B,F}) = 39.0$, $^2J(\text{B,F}) = 32.3$ Hz); FAB-MS: m/z (%): 97 (100) $[\text{C}_2\text{mim}]^+$, 137 (100) $[\text{CF}_3\text{BF}_3]^-$; elemental analysis calcd (%) for $\text{C}_6\text{H}_9\text{BF}_6\text{N}_2$ (234.95): C 30.8, H 3.9, N 12.0; found: C 30.5, H 4.0, N 11.9.

1-Ethyl-3-methylimidazolium trifluoromethyltrifluoroborate ($[\text{C}_2\text{mim}][\text{CF}_3\text{BF}_3]$): 85% yield, colorless liquid; $^1\text{H NMR}$: $\delta = 1.56$ (t, $J = 7.4$ Hz, 3H), 4.03 (s, 3H), 4.38 (q, $J = 7.3$ Hz, 2H), 7.67 (s, 1H), 7.74 (s, 1H), 8.94 ppm (s, 1H); $^{19}\text{F NMR}$: $\delta = -74.9$ (q, $^2J(\text{B,F}) = 32.6$ Hz, 3F; CF_3), -155.3 ppm (q, $^1J(\text{B,F}) = 39.6$ Hz, 3F; BF_3); $^{11}\text{B NMR}$: $\delta = -0.46$ ppm (qq, $^1J(\text{B,F}) = 39.1$, $^2J(\text{B,F}) = 32.4$ Hz); FAB-MS: m/z (%): 111 (100) $[\text{C}_2\text{mim}]^+$, 137 (100) $[\text{CF}_3\text{BF}_3]^-$; elemental analysis calcd (%) for $\text{C}_7\text{H}_{11}\text{BF}_6\text{N}_2$ (247.98): C 33.9, H 4.5, N 11.3; found: C 33.9, H 4.4, N 11.4.

1-Methyl-3-*n*-propylimidazolium trifluoromethyltrifluoroborate ($[\text{C}_3\text{mim}][\text{CF}_3\text{BF}_3]$): 88% yield, colorless liquid; $^1\text{H NMR}$: $\delta = 0.96$ (t, $J = 7.2$ Hz, 3H), 1.98 (m, 2H), 4.06 (s, 3H), 4.32 (t, $J = 7.3$ Hz, 2H), 7.71 (s, 1H), 7.75 (s, 1H), 8.98 ppm (s, 1H); $^{19}\text{F NMR}$: $\delta = -74.8$ (q, $^2J(\text{B,F}) = 32.6$ Hz, 3F; CF_3), -155.3 ppm (q, $^1J(\text{B,F}) = 38.6$ Hz, 3F; BF_3); $^{11}\text{B NMR}$: $\delta = -0.45$ ppm (qq, $^1J(\text{B,F}) = 38.8$, $^2J(\text{B,F}) = 32.3$ Hz); FAB-MS: m/z (%): 125 (100) $[\text{C}_3\text{mim}]^+$, 137 (100) $[\text{CF}_3\text{BF}_3]^-$; elemental analysis calcd (%) for $\text{C}_8\text{H}_{13}\text{BF}_6\text{N}_2$ (262.00): C 36.7, H 5.0, N 10.7; found: C 36.5, H 5.1, N 10.8.

1-Ethyl-3-*n*-butylimidazolium trifluoromethyltrifluoroborate ($[\text{C}_4\text{mim}][\text{CF}_3\text{BF}_3]$): 90% yield, colorless liquid; $^1\text{H NMR}$: $\delta = 0.95$ (t, $J = 7.2$ Hz, 3H), 1.40 (m, 2H), 1.93 (m, 2H), 4.04 (s, 3H), 4.35 (q, $J = 7.3$ Hz, 2H), 7.68 (s, 1H), 7.74 (s, 1H), 8.95 ppm (s, 1H); $^{19}\text{F NMR}$: $\delta = -74.8$ (q, $^2J(\text{B,F}) = 32.4$ Hz, 3F; CF_3), -155.2 ppm (q, $^1J(\text{B,F}) = 39.7$ Hz, 3F; BF_3); $^{11}\text{B NMR}$: $\delta = -0.45$ ppm (qq, $^1J(\text{B,F}) = 39.7$, $^2J(\text{B,F}) = 32.3$ Hz); FAB-MS: m/z (%): 139 (100) $[\text{C}_4\text{mim}]^+$, 137 (100) $[\text{CF}_3\text{BF}_3]^-$; elemental analysis calcd (%) for $\text{C}_9\text{H}_{15}\text{BF}_6\text{N}_2$ (276.03): C 39.2, H 5.5, N 10.2; found: C 38.9, H 5.8, N 10.2.

1-Ethyl-3-*n*-hexylimidazolium trifluoromethyltrifluoroborate ($[\text{C}_6\text{mim}][\text{CF}_3\text{BF}_3]$): 92% yield, colorless liquid; $^1\text{H NMR}$: $\delta = 0.87$ (t, $J = 7.0$ Hz, 3H), 1.34 (m, 3×2 H), 1.95 (m, 2H), 4.04 (s, 3H), 4.35 (t, $J = 7.2$ Hz, 2H), 7.69 (s, 1H), 7.75 (s, 1H), 8.97 ppm (s, 1H); $^{19}\text{F NMR}$: $\delta = -74.8$ (q, $^2J(\text{B,F}) = 32.6$ Hz, 3F; CF_3), -155.2 ppm (q, $^1J(\text{B,F}) = 39.6$ Hz, 3F; BF_3); $^{11}\text{B NMR}$: $\delta = -0.45$ ppm (qq, $^1J(\text{B,F}) = 38.9$, $^2J(\text{B,F}) = 32.0$ Hz); FAB-MS: m/z (%): 167 (100) $[\text{C}_6\text{mim}]^+$, 137 (100) $[\text{CF}_3\text{BF}_3]^-$; elemental analysis calcd (%) for $\text{C}_{11}\text{H}_{19}\text{BF}_6\text{N}_2$ (304.08): C 43.5, H 6.3, N 9.2; found: C 43.2, H 6.0, N 9.3.

1-Methoxymethyl-3-methylimidazolium trifluoromethyltrifluoroborate ($[\text{C}_2\text{Omim}][\text{CF}_3\text{BF}_3]$): 60% yield, colorless liquid; $^1\text{H NMR}$: $\delta = 3.44$ (s, 3H), 4.09 (s, 3H), 5.66 (s, 2H), 7.75 (s, 1H), 7.81 (s, 1H), 9.10 ppm (s, 1H); $^{19}\text{F NMR}$: $\delta = -74.9$ (q, $^2J(\text{B,F}) = 32.0$ Hz, 3F; CF_3), -155.1 ppm (q, $^1J(\text{B,F}) = 39.6$ Hz, 3F; BF_3); $^{11}\text{B NMR}$: $\delta = -0.46$ ppm (qq, $^1J(\text{B,F}) = 39.7$, $^2J(\text{B,F}) = 32.3$ Hz); FAB-MS: m/z (%): 127 (100) $[\text{C}_2\text{Omim}]^+$, 137 (100) $[\text{CF}_3\text{BF}_3]^-$; elemental analysis calcd (%) for $\text{C}_7\text{H}_{11}\text{BF}_6\text{N}_2\text{O}$ (263.98): C 31.9, H 4.2, N 10.6; found: C 31.7, H 4.3, N 10.6.

1-(2-Methoxyethyl)-3-methylimidazolium trifluoromethyltrifluoroborate ($[\text{C}_3\text{Omim}][\text{CF}_3\text{BF}_3]$): 63% yield, pale yellow liquid; $^1\text{H NMR}$: $\delta = 3.35$ (s, 3H), 3.81 (t, $J = 4.8$ Hz, 2H), 4.06 (s, 3H), 4.51 (t, $J = 4.8$ Hz, 2H), 7.67 (s, 1H), 7.70 (s, 1H), 8.94 ppm (s, 1H); $^{19}\text{F NMR}$: $\delta = -74.9$ (q, $^2J(\text{B,F}) = 32.4$ Hz, 3F; CF_3), -155.3 ppm (q, $^1J(\text{B,F}) = 38.6$ Hz, 3F; BF_3); $^{11}\text{B NMR}$: $\delta = -0.46$ ppm (qq, $^1J(\text{B,F}) = 38.8$, $^2J(\text{B,F}) = 32.3$ Hz); FAB-MS: m/z (%): 141 (100) $[\text{C}_3\text{Omim}]^+$, 137 (100) $[\text{CF}_3\text{BF}_3]^-$; elemental analysis calcd (%) for $\text{C}_8\text{H}_{13}\text{BF}_6\text{N}_2\text{O}$ (278.00): C 34.6, H 4.7, N 10.1; found: C 34.4, H 4.8, N 10.1.

1-[2-(2-Methoxyethoxy)ethyl]-3-methylimidazolium trifluoromethyltrifluoroborate ($[\text{C}_5\text{O}_2\text{mim}][\text{CF}_3\text{BF}_3]$): 63% yield, pale yellow liquid; $^1\text{H NMR}$: $\delta = 3.30$ (s, 3H), 3.49 (t, $J = 4.8$ Hz, 2H), 3.64 (t, $J = 4.6$ Hz, 2H), 3.91 (t, $J = 4.8$ Hz, 2H), 4.06 (s, 3H), 4.51 (t, $J = 4.6$ Hz, 2H), 7.68 (s, 1H), 7.73 (s, 1H), 8.96 ppm (s, 1H); $^{19}\text{F NMR}$: $\delta = -74.8$ (q, $^2J(\text{B,F}) = 32.6$ Hz, 3F; CF_3), -155.3 ppm (q, $^1J(\text{B,F}) = 38.7$ Hz, 3F; BF_3); $^{11}\text{B NMR}$: $\delta = -0.46$ ppm (qq, $^1J(\text{B,F}) = 39.7$, $^2J(\text{B,F}) = 33.1$ Hz); FAB-MS: m/z (%): 185 (100) $[\text{C}_5\text{O}_2\text{mim}]^+$, 137 (100) $[\text{CF}_3\text{BF}_3]^-$; elemental analysis calcd (%) for $\text{C}_{10}\text{H}_{17}\text{BF}_6\text{N}_2\text{O}_2$ (322.06): C 37.3, H 5.3, N 8.7; found: C 37.3, H 5.7, N 8.9.

1,3-Dimethylimidazolium pentafluoroethyltrifluoroborate ($[\text{C}_2\text{mim}][\text{C}_2\text{F}_5\text{BF}_3]$): 77% yield, pale yellow liquid; $^1\text{H NMR}$: $\delta = 4.05$ (s, 2×3 H), 7.67 (s, 2H), 8.91 ppm (s, 1H); $^{19}\text{F NMR}$: $\delta = -83.2$ (s, 3F; CF_3), -136.0 (q, $^2J(\text{B,F}) = 19.3$ Hz, 2F; CF_2), -153.0 ppm (q, $^1J(\text{B,F}) = 41.7$ Hz, 3F; BF_3); $^{11}\text{B NMR}$: $\delta = 0.23$ ppm (qt, $^1J(\text{B,F}) = 39.7$, $^2J(\text{B,F}) = 19.5$ Hz); FAB-MS: m/z (%): 97 (100) $[\text{C}_2\text{mim}]^+$, 187 (100) $[\text{C}_2\text{F}_5\text{BF}_3]^-$; elemental analysis calcd (%) for $\text{C}_7\text{H}_9\text{BF}_8\text{N}_2$ (283.96): C 29.6, H 3.2, N 9.9; found: C 29.2, H 3.2, N 9.8.

1-Ethyl-3-methylimidazolium pentafluoroethyltrifluoroborate ($[\text{C}_2\text{mim}][\text{C}_2\text{F}_5\text{BF}_3]$): 85% yield, colorless liquid; $^1\text{H NMR}$: $\delta = 1.55$ (t, $J = 7.4$ Hz, 3H), 4.03 (s, 3H), 4.38 (q, $J = 7.3$ Hz, 2H), 7.67 (s, 1H), 7.75 (s, 1H), 8.96 ppm (s, 1H); $^{19}\text{F NMR}$: $\delta = -83.2$ (s, 3F; CF_3), -136.0 (q, $^2J(\text{B,F}) = 19.3$ Hz, 2F; CF_2), -153.0 ppm (q, $^1J(\text{B,F}) = 41.7$ Hz, 3F; BF_3); $^{11}\text{B NMR}$: $\delta = 0.23$ ppm (qt, $^1J(\text{B,F}) = 40.9$, $^2J(\text{B,F}) = 19.9$ Hz); FAB-MS: m/z (%): 111 (100) $[\text{C}_2\text{mim}]^+$, 187 (100) $[\text{C}_2\text{F}_5\text{BF}_3]^-$; elemental analysis calcd (%) for $\text{C}_8\text{H}_{11}\text{BF}_8\text{N}_2$ (297.98): C 32.3, H 3.7, N 9.4; found: C 32.3, H 3.8, N 9.3.

1-Methyl-3-*n*-propylimidazolium pentafluoroethyltrifluoroborate ($[\text{C}_3\text{mim}][\text{C}_2\text{F}_5\text{BF}_3]$): 89% yield, colorless liquid; $^1\text{H NMR}$: $\delta = 0.96$ (t, $J = 7.4$ Hz, 3H), 1.98 (m, 2H), 4.05 (s, 3H), 4.31 (t, $J = 7.2$ Hz, 2H), 7.69 (s, 1H), 7.74 (s, 1H), 8.96 ppm (s, 1H); $^{19}\text{F NMR}$: $\delta = -83.2$ (s, 3F; CF_3), -136.0 (q, $^2J(\text{B,F}) = 19.3$ Hz, 2F; CF_2), -152.8 ppm (q, $^1J(\text{B,F}) = 40.6$ Hz, 3F; BF_3); $^{11}\text{B NMR}$: $\delta = 0.25$ ppm (qt, $^1J(\text{B,F}) = 40.9$, $^2J(\text{B,F}) = 19.1$ Hz); FAB-MS: m/z (%): 125 (100) $[\text{C}_3\text{mim}]^+$, 187 (100) $[\text{C}_2\text{F}_5\text{BF}_3]^-$; elemental analysis calcd (%) for $\text{C}_9\text{H}_{13}\text{BF}_8\text{N}_2$ (312.01): C 34.7, H 4.2, N 9.0; found: C 34.6, H 4.4, N 9.2.

1-Ethyl-3-*n*-butylimidazolium pentafluoroethyltrifluoroborate ($[\text{C}_4\text{mim}][\text{C}_2\text{F}_5\text{BF}_3]$): 91% yield, colorless liquid; $^1\text{H NMR}$: $\delta = 0.93$ (t, $J = 7.4$ Hz, 3H), 1.37 (m, 2H), 1.91 (m, 2H), 4.02 (s, 3H), 4.33 (q, $J = 7.0$ Hz, 2H), 7.67 (s, 1H), 7.72 (s, 1H), 8.93 ppm (s, 1H); $^{19}\text{F NMR}$: $\delta = -83.2$ (s, 3F; CF_3), -136.0 (q, $^2J(\text{B,F}) = 19.3$ Hz, 2F; CF_2), -152.8 ppm (q, $^1J(\text{B,F}) = 40.6$ Hz, 3F; BF_3); $^{11}\text{B NMR}$: $\delta = 0.25$ ppm (qt, $^1J(\text{B,F}) = 40.9$, $^2J(\text{B,F}) = 19.9$ Hz); FAB-MS: m/z (%): 139 (100) $[\text{C}_4\text{mim}]^+$, 187 (100) $[\text{C}_2\text{F}_5\text{BF}_3]^-$;

elemental analysis calcd (%) for $C_{10}H_{15}BF_8N_2$ (326.04): C 36.8, H 4.6, N 8.6; found: C 36.7, H 4.7, N 8.7.

1-Ethyl-3-*n*-hexylimidazolium pentafluoroethyltrifluoroborate ([C₆mim][C₂F₅BF₃]): 94% yield, colorless liquid; ¹H NMR: δ = 0.87 (t, *J* = 7.0 Hz, 3H), 1.34 (m, 3 × 2H), 1.95 (m, 2H), 4.04 (s, 3H), 4.35 (t, *J* = 7.2 Hz, 2H), 7.68 (s, 1H), 7.75 (s, 2H), 8.96 ppm (s, 1H); ¹⁹F NMR: δ = -83.1 (s, 3F; CF₃), -136.0 (q, ²*J*(B,F) = 19.3 Hz, 2F; CF₂), -153.0 ppm (q, ¹*J*(B,F) = 40.6 Hz, 3F; BF₃); ¹¹B NMR: δ = 0.25 ppm (qt, ¹*J*(B,F) = 40.9, ²*J*(B,F) = 19.9 Hz); FAB-MS: *m/z* (%): 167 (100) [C₆mim]⁺, 187 (100) [C₂F₅BF₃]⁻; elemental analysis calcd (%) for C₁₂H₁₉BF₈N₂ (354.09): C 40.7, H 5.4, N 7.9; found: C 40.7, H 5.1, N 7.9.

1-Methoxyethyl-3-methylimidazolium pentafluoroethyltrifluoroborate ([C₂Omim][C₂F₅BF₃]): 65% yield, colorless liquid; ¹H NMR: δ = 3.44 (s, 3H), 4.09 (s, 3H), 5.66 (s, 2H), 7.75 (s, 1H), 7.82 (s, 1H), 9.11 ppm (s, 1H); ¹⁹F NMR: δ = -83.2 (s, 3F; CF₃), -136.0 (q, ²*J*(B,F) = 20.3 Hz, 2F; CF₂), -152.8 ppm (q, ¹*J*(B,F) = 40.6 Hz, 3F; BF₃); ¹¹B NMR: δ = 0.23 ppm (qt, ¹*J*(B,F) = 40.9, ²*J*(B,F) = 19.9 Hz); FAB-MS: *m/z* (%): 127 (100) [C₂Omim]⁺, 187 (100) [C₂F₅BF₃]⁻; elemental analysis calcd (%) for C₈H₁₁BF₈N₂O (313.98): C 30.6, H 3.5, N 8.9; found: C 30.5, H 3.6, N 9.0.

1-(2-Methoxyethyl)-3-methylimidazolium pentafluoroethyltrifluoroborate ([C₃Omim][C₂F₅BF₃]): 65% yield, pale yellow liquid; ¹H NMR: δ = 3.35 (s, 3H), 3.81 (t, *J* = 4.8 Hz, 2H), 4.05 (s, 3H), 4.51 (t, *J* = 4.6 Hz, 2H), 7.67 (s, 1H), 7.71 (s, 1H), 8.94 ppm (s, 1H); ¹⁹F NMR: δ = -83.1 (s, 3F; CF₃), -136.0 (q, ²*J*(B,F) = 19.3 Hz, 2F; CF₂), -153.0 ppm (q, ¹*J*(B,F) = 40.7 Hz, 3F; BF₃); ¹¹B NMR: δ = 0.23 ppm (qt, ¹*J*(B,F) = 40.9, ²*J*(B,F) = 19.9 Hz); FAB-MS: *m/z* (%): 141 (100) [C₃Omim]⁺, 187 (100) [C₂F₅BF₃]⁻; elemental analysis calcd (%) for C₉H₁₃BF₈N₂O (328.01): C 33.0, H 4.0, N 8.5; found: C 32.9, H 3.9, N 8.9.

1-[2-(2-Methoxyethoxy)ethyl]-3-methylimidazolium pentafluoroethyltrifluoroborate ([C₅O₂mim][C₂F₅BF₃]): 68% yield, pale yellow liquid; ¹H NMR: δ = 3.30 (s, 3H), 3.49 (t, *J* = 4.6 Hz, 2H), 3.64 (t, *J* = 4.6 Hz, 2H), 3.91 (t, *J* = 4.6 Hz, 2H), 4.06 (s, 3H), 4.51 (t, *J* = 4.6 Hz, 2H), 7.68 (s, 1H), 7.74 (s, 1H), 8.97 ppm (s, 1H); ¹⁹F NMR: δ = -83.1 (s, 3F; CF₃), -135.9 (q, ²*J*(B,F) = 19.3 Hz, 2F; CF₂), -153.1 ppm (q, ¹*J*(B,F) = 40.6 Hz, 3F; BF₃); ¹¹B NMR: δ = 0.23 ppm (qt, ¹*J*(B,F) = 40.9, ²*J*(B,F) = 19.9 Hz); FAB-MS: *m/z* (%): 185 (100) [C₅O₂mim]⁺, 187 (100) [C₂F₅BF₃]⁻; elemental analysis calcd (%) for C₁₁H₁₇BF₈N₂O₂ (372.06): C 35.5, H 4.6, N 7.5; found: C 35.3, H 4.6, N 7.7.

1,3-Dimethylimidazolium (heptafluoro-*n*-propyl)trifluoroborate ([C₁mim][nC₃F₇BF₃]): 88% yield, pale yellow liquid; ¹H NMR: δ = 4.05 (s, 2 × 3H), 7.67 (s, 2H), 8.91 ppm (s, 1H); ¹⁹F NMR: δ = -80.6 (s, 3F; CF₃), -127.7 (s, 2F; BCCF₂-), -133.9 (s, 2F; CF₂B), -152.4 ppm (q, ¹*J*(B,F) = 39.6 Hz, 3F; BF₃); ¹¹B NMR: δ = 0.27 ppm (qt, ¹*J*(B,F) = 40.9, ²*J*(B,F) = 19.1 Hz); FAB-MS: *m/z* (%): 97 (100) [C₁mim]⁺, 237 (100) [C₃F₇BF₃]⁻; elemental analysis calcd (%) for C₈H₉BF₁₀N₂ (333.97): C 28.8, H 2.7, N 8.4; found: C 28.8, H 2.8, N 8.2.

1-Ethyl-3-methylimidazolium (heptafluoro-*n*-propyl)trifluoroborate ([C₂mim][nC₃F₇BF₃]): 90% yield, colorless liquid; ¹H NMR: δ = 1.56 (t, *J* = 7.4 Hz, 3H), 4.04 (s, 3H), 4.38 (q, *J* = 7.3 Hz, 2H), 7.67 (s, 1H), 7.75 (s, 1H), 8.96 ppm (s, 1H); ¹⁹F NMR: δ = -80.6 (s, 3F; CF₃), -127.6 (s, 2F; BCCF₂-), -133.8 (s, 2F; CF₂B), -152.4 ppm (q, ¹*J*(B,F) = 40.6 Hz, 3F; BF₃); ¹¹B NMR: δ = 0.27 ppm (qt, ¹*J*(B,F) = 40.9, ²*J*(B,F) = 19.1 Hz); FAB-MS: *m/z* (%): 111 (100) [C₂mim]⁺, 237 (100) [C₃F₇BF₃]⁻; elemental analysis calcd (%) for C₉H₁₁BF₁₀N₂ (347.99): C 31.1, H 3.2, N 8.1; found: C 31.0, H 3.3, N 8.3.

1-Methy-3-*n*-propylimidazolium (heptafluoro-*n*-propyl)trifluoroborate ([C₃mim][nC₃F₇BF₃]): 92% yield, colorless liquid; ¹H NMR: δ = 0.96 (t, *J* = 7.4 Hz, 3H), 1.97 (m, 2H), 4.05 (s, 3H), 4.32 (t, *J* = 7.2 Hz, 2H), 7.70 (s, 1H), 7.75 (s, 1H), 8.97 ppm (s, 1H); ¹⁹F NMR: δ = -80.6 (s, 3F; CF₃), -127.6 (s, 2F; BCCF₂-), -133.8 (s, 2F; CF₂B), -152.4 ppm (q, ¹*J*(B,F) = 40.7 Hz, 3F; BF₃); ¹¹B NMR: δ = 0.28 ppm (qt, ¹*J*(B,F) = 40.9, ²*J*(B,F) = 19.1 Hz); FAB-MS: *m/z* (%): 125 (100) [C₃mim]⁺, 237 (100) [C₃F₇BF₃]⁻; elemental analysis calcd (%) for C₁₀H₁₃BF₁₀N₂ (362.02): C 33.2, H 3.6, N 7.7; found: C 33.0, H 3.6, N 7.7.

1,3-Dimethylimidazolium (nonafluoro-*n*-butyl)trifluoroborate ([C₁mim][nC₄F₉BF₃]): 90% yield, white solid; ¹H NMR: δ = 4.03 (s, 2 × 3H), 7.66 (s, 2H), 8.88 ppm (s, 1H); ¹⁹F NMR: δ = -80.9 (s, 3F; CF₃), -123.9 (s, 2F; BCCF₂-), -125.9 (s, 2F; BCCF₂-), -133.2 (s, 2F; CF₂B), -152.0 ppm (q, ¹*J*(B,F) = 39.7 Hz, 3F; BF₃); ¹¹B NMR: δ = 0.28 ppm (qt, ¹*J*(B,F) = 40.9, ²*J*(B,F) = 19.1 Hz); FAB-MS: *m/z* (%): 97 (100) [C₁mim]⁺,

287 (100) [C₄F₉BF₃]⁻; elemental analysis calcd (%) for C₉H₉BF₁₂N₂ (383.97): C 28.2, H 2.4, N 7.3; found: C 28.2, H 2.2, N 7.1.

1-Ethyl-3-methylimidazolium (nonafluoro-*n*-butyl)trifluoroborate ([C₂mim][nC₄F₉BF₃]): 92% yield, colorless liquid; ¹H NMR: δ = 1.56 (t, *J* = 7.4 Hz, 3H), 4.04 (s, 3H), 4.38 (q, *J* = 7.3 Hz, 2H), 7.67 (s, 1H), 7.75 (s, 1H), 8.96 ppm (s, 1H); ¹⁹F NMR: δ = -80.6 (s, 3F; CF₃), -123.9 (s, 2F; BCCF₂-), -125.9 (s, 2F; BCCF₂-), -133.2 (s, 2F; CF₂B), -152.1 ppm (q, ¹*J*(B,F) = 40.7 Hz, 3F; BF₃); ¹¹B NMR: δ = 0.29 ppm (qt, ¹*J*(B,F) = 40.6, ²*J*(B,F) = 19.1 Hz); FAB-MS: *m/z* (%): 111 (100) [C₂mim]⁺, 287 (100) [C₄F₉BF₃]⁻; elemental analysis calcd (%) for C₁₀H₁₁BF₁₂N₂ (398.00): C 30.2, H 2.8, N 7.0; found: C 30.0, H 2.8, N 7.1.

1-Methy-3-*n*-propylimidazolium (nonafluoro-*n*-butyl)trifluoroborate ([C₃mim][nC₄F₉BF₃]): 95% yield, colorless liquid; δ = 0.96 (t, *J* = 7.4 Hz, 3H), 1.97 (m, 2H), 4.05 (s, 3H), 4.32 (t, *J* = 7.2 Hz, 2H), 7.70 (s, 1H), 7.75 (s, 1H), 8.98 ppm (s, 1H); ¹⁹F NMR: δ = -80.6 (s, 3F; CF₃), -123.9 (s, 2F; BCCF₂-), -125.9 (s, 2F; BCCF₂-), -133.2 (s, 2F; CF₂B), -152.1 ppm (q, ¹*J*(B,F) = 40.7 Hz, 3F; BF₃); ¹¹B NMR: δ = 0.29 ppm (qt, ¹*J*(B,F) = 40.6, ²*J*(B,F) = 19.1 Hz); FAB-MS: *m/z* (%): 125 (100) [C₃mim]⁺, 287 (100) [C₄F₉BF₃]⁻; elemental analysis calcd (%) for C₁₁H₁₃BF₁₂N₂ (412.03): C 32.1, H 3.2, N 6.8; found: C 32.0, H 3.2, N 6.9.

Acknowledgement

This work was supported by R&D project for Li batteries by METI and NEDO of Japan. We thank Ms. Kazuko Igarashi and Ms. Etsuko Hazama for their assistances to this work.

- a) D. Holbrey, K. R. Seddon, *Clean Prod. Process* **1999**, *1*, 223–236; b) T. Welton, *Chem. Rev.* **1999**, *99*, 2071–2084; c) P. Wasserscheid, W. Keim, *Angew. Chem.* **2000**, *112*, 3926–3945; *Angew. Chem. Int. Ed.* **2000**, *39*, 3772–3789; d) H. Olivier-Bourbigou, L. Magna, *J. Mol. Catal. A* **2002**, *183*, 419–437; e) J. Dupont, R. F. de Souza, P. A. Z. Suarez, *Chem. Rev.* **2002**, *102*, 3667–3692; f) J. S. Wilkes, *J. Mol. Catal. A* **2004**, *214*, 11–17.
- a) R. A. Sheldon, R. M. Lau, M. J. Sorgedragger, F. van-Rantwijk, K. R. Seddon, *Green Chem.* **2002**, *4*, 147–151; b) U. Kragel, M. Eckstein, N. Kaftzik, *Curr. Opin. Biotechnol.* **2002**, *13*, 565–571; c) S. Park, R. J. Kazlauskas, *Curr. Opin. Biotechnol.* **2003**, *14*, 432–437; d) F. van Rantwijk, R. M. Lau, R. A. Sheldon, *Trends Biotechnol.* **2003**, *21*, 131–138.
- a) C. Tzschucke, C. Markert, W. Bannwarth, S. Roller, A. Hebel, R. Haag, *Angew. Chem.* **2002**, *114*, 4136–4173; *Angew. Chem. Int. Ed.* **2002**, *41*, 3964–4000; b) S. V. Dzyuba, R. A. Bartsch, *Angew. Chem.* **2003**, *115*, 158–160; *Angew. Chem. Int. Ed.* **2003**, *42*, 148–150; c) C. F. Poole, *J. Chromatogr. A* **2004**, *1037*, 49–82.
- a) A. Weber, G. E. Blomgren in *Advances in Lithium-Ion Batteries* (Eds.: W. A. Van Schalkwijk, B. Scrosati), Kluwer Academic/Plenum Publishers, New York, **2002**, pp. 185–232; b) D. R. MacFarlane, M. Forsyth, *Adv. Mater.* **2001**, *13*, 957–966; c) R. Hagiwara, Y. Ito, *J. Fluorine Chem.* **2000**, *105*, 221–227; d) F. Endres, *ChemPhysChem* **2002**, *3*, 144–154.
- D. M. Fox, W. H. Awad, J. W. Gilman, P. H. Maupin, H. C. De Long, P. C. Trulove, *Green Chem.* **2003**, *5*, 724–727.
- D. Behar, C. Gonnzalez, P. Neta, *J. Phys. Chem. A* **2001**, *105*, 7607–7614.
- A. F. Fannin, D. A. Floreani, L. A. King, J. S. Landers, B. J. Piersma, D. J. Stech, R. L. Vaughn, J. S. Wilkes, J. L. Williams, *J. Phys. Chem.* **1984**, *88*, 2614–2621.
- a) R. Hagiwara, T. Hirashige, T. Tsuda, Y. Ito, *J. Fluorine Chem.* **1999**, *99*, 1–3; b) R. Hagiwara, T. Hirashige, T. Tsuda, Y. Ito, *J. Electrochem. Soc.* **2002**, *149*, D1–D6; c) R. Hagiwara, K. Matsumoto, Y. Nakamori, T. Tsuda, Y. Ito, H. Matsumoto, K. Momota, *J. Electrochem. Soc.* **2003**, *150*, D195–D199.
- a) D. R. MacFarlane, J. Golding, S. Forsyth, M. Forsyth, G. B. Deacon, *Chem. Commun.* **2001**, 1430–1431; b) D. R. MacFarlane, S. A. Forsyth, J. Golding, G. B. Deacon, *Green Chem.* **2002**, *4*, 444–448.

- [10] Y. Yoshida, K. Muroi, A. Otsuka, G. Saito, M. Takahashi, T. Yoko, *Inorg. Chem.* **2004**, *43*, 1458–1462.
- [11] S. A. Forsyth, S. R. Batten, Q. Dai, D. R. MacFarlane, *Aust. J. Chem.* **2004**, *57*, 121–124.
- [12] H. Matsumoto, H. Kageyama, Y. Miyazaki, *Chem. Commun.* **2002**, 1726–1727.
- [13] A. B. McEwen, H. L. Ngo, K. LeCompte, J. L. Goldman, *J. Electrochem. Soc.* **1999**, *146*, 1687–1695.
- [14] P. Bonhote, A. P. Dias, N. Papageorgiou, K. Kalyanasundaram, M. Graetzel, *Inorg. Chem.* **1996**, *35*, 1168–1178.
- [15] a) J. S. Wilkes, M. J. Zaworotko, *J. Chem. Soc. Chem. Commun.* **1992**, 965–967; b) J. Fuller, R. T. Carlin, R. A. Osteryoung, *J. Electrochem. Soc.* **1997**, *144*, 3881–3886; c) T. Nishida, Y. Tashiro, M. Yamamoto, *J. Fluorine Chem.* **2003**, *120*, 135–141.
- [16] a) K. Matsumoto, R. Hagiwara, R. Yoshida, Y. Ito, Z. Mazej, P. Benkic, B. Zemva, O. Tamada, H. Yoshino, S. Matsubara, *J. Chem. Soc. Dalton Trans.* **2004**, 144–149; b) H. Yoshino, S. Matsubara, K. Oshima, K. Matsumoto, R. Hagiwara, Y. Ito, *J. Fluorine Chem.* **2004**, *125*, 455–458.
- [17] J. D. Holbrey, K. R. Seddon, *J. Chem. Soc. Dalton Trans.* **1999**, 2133–2140.
- [18] R. F. de Souza, S. Einloft, J. E. L. Dullius, P. A. Z. Suarez, J. Dupont, *J. Chim. Phys. Phys. Chim. Biol.* **1998**, *95*, 1626–1639.
- [19] H. L. Ngo, K. LeCompte, L. Hargens, A. B. McEwen, *Thermochim. Acta* **2000**, *357/358*, 97–102.
- [20] J. G. Huddleston, A. E. Visser, W. M. Reichert, H. D. Willauer, G. A. Broker, R. D. Rogers, *Green Chem.* **2001**, *3*, 156–164.
- [21] a) K. R. Seddon, A. Stark, M. J. Torres, *Pure Appl. Chem.* **2000**, *72*, 2275–2287; b) M. J. Muldoon, C. M. Gordon, I. R. Dunkin, *J. Chem. Soc. Perkin Trans. 2* **2001**, 433–435; c) C. Villagrana, C. E. Banks, C. Hardacre, R. G. Compton, *Anal. Chem.* **2004**, *76*, 1998–2003; d) C. Villagran, M. Deetlefs, W. R. Pitner, C. Hardacre, *Anal. Chem.* **2004**, *76*, 2118–2123.
- [22] a) V. Gallo, P. Mastrorilli, C. F. Nobile, G. Romanazzi, G. P. Suranna, *J. Chem. Soc. Dalton Trans.* **2002**, 4339–4342; b) S. Park, R. J. Kazlauskas, *J. Org. Chem.* **2001**, *66*, 8395–8401.
- [23] H. J. Frohn, V. V. Bardin, *Z. Anorg. Allg. Chem.* **2001**, *627*, 15–16.
- [24] Z. B. Zhou, M. Takeda, M. Ue, *J. Fluorine Chem.* **2003**, *123*, 127–131.
- [25] A. A. Kolomeitsev, A. A. Kadyrov, J. Szczepkowska-Sztolcman, M. Milewska, H. Koroniak, G. Bissky, J. A. Barten, G. V. Roschenthaler, *Tetrahedron Lett.* **2003**, *44*, 8273–8277.
- [26] G. A. Molander, B. P. Hoag, *Organometallics* **2003**, *22*, 3313–3315.
- [27] a) V. V. Bardin, H. J. Frohn, *Main Group Met. Chem.* **2002**, *25*, 589–613; b) G. Pawelke, H. Bürger, *Coord. Chem. Rev.* **2001**, *215*, 243–266.
- [28] a) V. V. Bardin, S. G. Idemskaya, H. J. Frohn, *Z. Anorg. Allg. Chem.* **2002**, *628*, 883–890; b) M. Takeda, M. Takehara, M. Ue (Mitsubishi Chem.), JP 63934A, **2002**; c) M. Schmidt, A. Kuhner, K.-D. Franz, G.-V. Roschenthaler, G. Bissky, A. Kolomeitsev, A. Kadyrov (Merck GmbH), US 0160261 A1, **2002**.
- [29] a) Z. B. Zhou, M. Takeda, M. Ue, *J. Fluorine Chem.* **2004**, *125*, 471–476; b) Z. B. Zhou, H. Matsumoto, K. Tatsumi, *Chem. Lett.* **2004**, 680–681.
- [30] L. C. Branco, J. N. Rosa, J. J. M. Ramos, C. A. M. Afonso, *Chem. Eur. J.* **2002**, *8*, 3671–3677.
- [31] D. R. MacFarlane, P. Meakin, J. Sun, N. Amini, M. Forsyth, *J. Phys. Chem. B* **1999**, *103*, 4164–4170.
- [32] a) S. V. Dzyuba, R. A. Bartsch, *Chem. Commun.* **2001**, 1466–1467; b) S. V. Dzyuba, R. A. Bartsch, *ChemPhysChem* **2002**, *3*, 161–166; c) A. S. Larsen, J. D. Holbrey, F. S. Tham, C. A. Reed, *J. Am. Chem. Soc.* **2000**, *122*, 7264–7272; d) D. Zhao, Z. Fei, R. Scopelliti, P. J. Dyson, *Inorg. Chem.* **2004**, *43*, 2197–2205.
- [33] a) S. Hayashi, R. Ozawa, H. Hamaguchi, *Chem. Lett.* **2003**, 498–499; b) J. D. Holbrey, W. M. Reichert, M. Nieuwenhuyzen, S. Johnston, K. R. Seddon, R. D. Rogers, *Chem. Commun.* **2003**, 1636–1637.
- [34] M. Ue, M. Takeda, A. Toriumi, A. Kominato, R. Hagiwara, Y. Ito, *J. Electrochem. Chem.* **2003**, *150*, A499–A502.
- [35] P. Walden, *Z. Phys. Chem.* **1912**, *78*, 257–283.
- [36] G. Gritzner, J. Kuta, *Pure Appl. Chem.* **1984**, *56*, 461–466.
- [37] a) H. Matsumoto, M. Yanagida, K. Tanimoto, M. Nomura, Y. Kitagawa, Y. Miyazaki, *Chem. Lett.* **2000**, 922–923; b) M. Ue, M. Takeda, *J. Korean Electrochem. Soc.* **2002**, *5*, 192–196.
- [38] U. Schroder, J. D. Wadhawan, R. G. Compton, F. Marken, P. A. Z. Suarez, C. S. Consorti, R. F. de Souza, J. Dupont, *New J. Chem.* **2000**, *12*, 1009–1015.
- [39] P. A. Z. Suarez, V. M. Selbach, J. E. L. Dullius, S. Einloft, C. M. S. Piatnicki, D. S. Azambuja, R. F. de Souza, J. DuPont, *Electrochim. Acta* **1997**, *42*, 2533–2535.

Received: May 28, 2004
Published online: November 11, 2004